JACS Au
AN OPEN ACCESS JOURNAL OF THE AMERICAN CHEMICAL SOCIETY

pubs.acs.org/jacsau
Perspective

Challenges and Opportunities of Functionalized Cucurbiturils for Biomedical Applications

Hang Yin,[#] Qian Cheng,[#] David Bardelang,[*] and Ruibing Wang[*]

Cite This: *JACS Au* 2023, 3, 2356−2377

Read Online

ACCESS | Metrics & More | Article Recommendations

ABSTRACT: Cucurbit[*n*]uril (CB[*n*]) macrocycles (especially CB[5] to CB[8]) have shown exceptional attributes since their discovery in 2000. Their stability, water solubility, responsiveness to several stimuli, and remarkable binding properties have enabled a growing number of biological applications. Yet, soon after their discovery, the challenge of their functionalization was set. Nevertheless, after more than two decades, a myriad of CB[*n*] derivatives has been described, many of them used in cells or in vivo for advanced applications. This perspective summarizes key advances of this burgeoning field and points to the next opportunities and remaining challenges to fully express the potential of these fascinating macrocycles in biology and biomedical sciences.

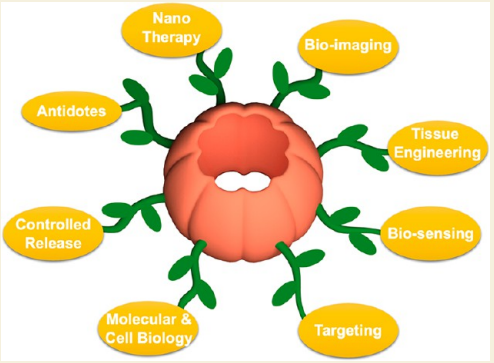

KEYWORDS: *Macrocycles, Cucurbiturils, Functionalization, Biomedical application, Supramolecular Biomaterials*

1. INTRODUCTION

Supramolecular chemistry has been developing tremendously for the past half-century. In this context, host•guest interactions based on macrocyclic molecules have attracted considerable attention.[1−5] Among the main families of macrocycles including cyclodextrins, calixarenes, and pillararenes, the family of cucurbit[*n*]urils (CB[*n*]s, *n* = 5−8, 10, 13−15) have developed since 2000 as an original class of macrocyclic compounds.[6−12] Their water solubility (especially for CB[7]), stimuli-responsiveness, and extraordinary binding properties toward a variety of guest species made them amenable for several biological applications.[13−17] For example, by forming inclusion complexes, (i) they can improve the solubility (and stability) of otherwise insoluble drugs permitting their use in biology (use as an excipient),[18,19] (ii) they can improve therapeutic efficacies and reduce side effects,[20,21] or (iii) they can be used as reversal agents for toxic molecules, when the binding is sufficiently high (i.e., paraquat).[22,23] In parallel, researchers realized soon after their discovery that their full potential could be unlocked if they could be functionalized. Indeed, the added value conferred by the attached groups could be combined with the unique properties of the CB[*n*] cavities to produce conjugates featuring synergistic properties. The literature is replete with examples of cyclodextrin,[24,25] calixarene,[26] or pillararene[27,28] derivatives, many of them used in biology and biomedical sciences.[25,26,29,30] For instance, the introduction of carboxyl thioether groups on γ-cyclodextrins dramatically improved the affinity of the host toward neuromuscular blocking agents (NMBAs).[31,32] Replacement of *tert*-butyl groups by sulfonates on calixarenes enhanced their water solubility and reduced their toxicity.[33] The functionalization of pillar[6]arenes by carboxylate groups improved both their water solubility and their affinity for paraquat.[27,34] However, CB[*n*] are quite chemically inert, and their functionalization has rapidly become a daunting task. Nevertheless, more than 30 CB[*n*] derivatives are known today, carrying either hydrophobic tails, hydrophilic groups, fluorescent tags, targeting units, or DNA strands, all of them used in biomedical applications. Even if improved methods of derivatization are still highly desirable to facilitate access to more functional CB[*n*] macrocycles, the ensemble of CB[*n*] derivatives reported up to now shows (i) that functionalized CB[*n*] is not structurally limited and (ii) that the grafted group imparts dramatic changes, often enabling the modified CB[*n*] to be applied in an entire new application or research field. In this Perspective, we have summarized the three main strategies enabling access to functionalized CB[*n*] (*F*-CB[*n*]) and reviewed recent advances in their applications (*F*-CB[5] to *F*-CB[8]) at the interface of chemistry and biology. Finally, we discuss key advances and

Received: May 30, 2023
Revised: July 9, 2023
Accepted: July 10, 2023
Published: August 28, 2023

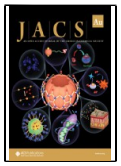

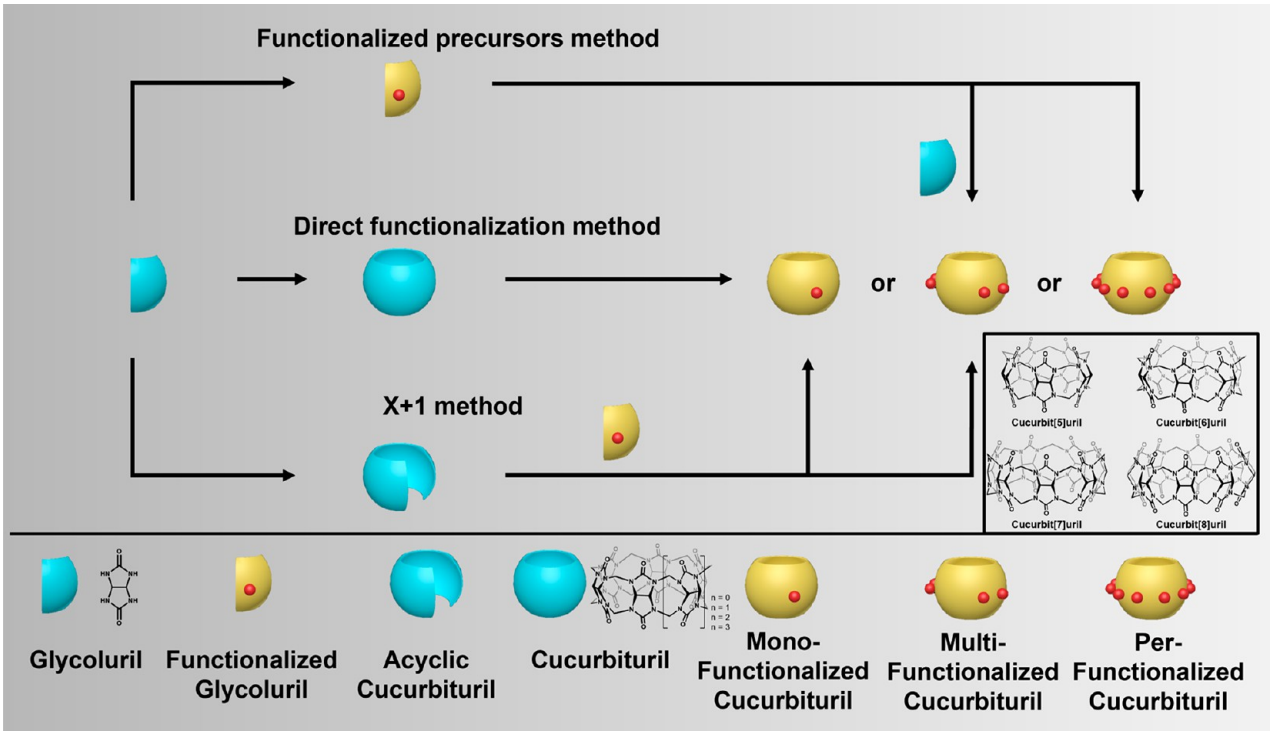

Figure 1. Schematic illustration of the three main strategies for the synthesis of *F*-CB[*n*]s.

propose next challenges to overcome, expected to create new opportunities for both supramolecular and biomedical fields.

2. MAIN METHODS TO PREPARE FUNCTIONALIZED CUCURBITURILS

Many efforts have been devoted to developing new synthesis methods for the preparation of *F*-CB[*n*]. Today, three main strategies are available to access these compounds[11] (Figure 1).

One of the most important aspects was to find a method featured by (i) ease of execution and (ii) high yields. Another perhaps equally important question is (iii) the need or the ease of purification. Each strategy possesses its own advantages and drawbacks, but it happened that the direct functionalization and the X+1 method were the most useful considering the number of *F*-CB[*n*] reported. The prefunctionalization (functionalized precursor method, considering modified glycolurils reacted with unmodified analogues) often yielded statistical mixtures or small-cavity macrocycles, less used in biology. The post- (or direct) functionalization or the X+1 method afforded many derivatives, the vast majority of which are monofunctionalized CB[*n*] which have been largely used in biomedical experiments.

2.1. Functionalized Precursors

In the classical CB[*n*] synthesis, glycoluril is condensed with formaldehyde to produce the ring-shape macrocycles (Figure 1).[35] Quite early in this field, researchers tried to modify the structure of the glycoluril monomer before cyclization. Tao and co-workers have prepared in this way a variety of *F*-CB[*n*]s featured by several (most often) hydrophobic groups on the carbon atoms in the equatorial plane of the hosts.[36] However, bifunctionalized glycolurils usually yield small cavity CB[*n*]s ($n \leq 6$) presumably due to deleterious steric effects hindering the formation of larger cavity ($n \geq 7$) macrocycles. Alternatively, mixtures of functionalized and unmodified glycoluril precursors, or monofunctionalized glycolurils yielded larger cavity *F*-CB[*n*].[37] Hemimethyl-substituted CB[7] (**HMeCB**[7]) is one of the notable *F*-CB[7] obtained from monofunctionalized glycoluril.[37] Compared to CB[7], **HMeCB**[7] (methyl groups are randomly distributed) showed higher water solubility and better biocompatibility in vitro and in vivo.[38] Therefore, efforts in this direction seem to have focused on modifying the glycoluril unit on the methine groups delivering *F*-CB[*n*] modified only on the macrocycle periphery. Another strategy could consist of elongating the glycoluril unit to produce *F*-CB[*n*] featured by higher cavities (from one carbonyl rim to the other) but constrains in the glycoluril geometry seem important to allow macrocyclization which could explain why such derivatives have not yet been described (i.e., inheritance angle[39] and propensity for C-shape dimers versus S-shape dimers[40]).

2.2. Direct Functionalization

Postfunctionalization consists of directly modifying the structure of CB[*n*] with suitable functional groups (Figure 1).[41,42] However, due to the chemical inertness of these macrocycles, rather harsh conditions are required to modify them. Thus, it was particularly hard to work on the carbonyl (urea) functions or on the bridging methylene groups.[43] However, the outer C−H bonds were found to be particularly sensitive to oxidation. Kim and co-workers managed to transform CB[6] to perhydroxy CB[6] using $K_2S_2O_8$ in water at 85 °C.[41] Hydroxyl substituents could next be substituted by other functional (i.e., allyl) groups toward several *F*-CB[6], but this method was initially better to modify CB[5] and CB[6].[41] By modulating experimental conditions, monohydroxy CB[6] (**CB[6]-(OH)$_1$**)[44] and monohydroxy CB[7] (**CB[7]-(OH)$_1$**)[45] could be produced, the latter subsequently derivatized to monoallyloxy CB[7] by a Williamson reaction with a strong base.[45,46] Then, Kim and co-workers introduced another method from **CB[6]-(OH)$_1$** or **CB[7]-(OH)$_1$** to substitute the hydroxyl group by several

https://doi.org/10.1021/jacsau.3c00273
JACS Au 2023, 3, 2356−2377

nitriles or alcohols in superacidic conditions.[47] In parallel, a mild oxidation reaction was set for CB[*n*] to get **CB[*n*]-(OH)$_1$** (*n* = 5 to 8) using the homolytic cleavage of H_2O_2 by UV light (254 nm) in acidic water.[42] Even if isolated yields of monohydroxylation remain rather modest (between ∼5 and 30% depending on the CB[*n*] considered),[45,48] the direct hydroxylation methods have started to be largely used worldwide.[49−52] More recently, carborane guest molecules that can be controllably included in CB[7] have been used to facilitate the isolation of **CB[7]-(OH)$_1$**,[53] which appeared to be a key compound to access a growing family of monofunctionalized *F*-CB[7].

2.3. X+1 Method

In parallel, Isaacs and co-workers introduced a building-block approach to access a series of monofunctional CB[6][54] and CB[7][55] derivatives (Figure 1). After isolation of C-shape acyclic CB[*n*]-type molecules, especially a glycoluril hexamer,[56] this team managed to prepare mono-*F*-CB[*n*] by coupling glycoluril hexamers with relevant building blocks (often a monofunctionalized glycoluril unit).[55] A growing ensemble of mono-*F*-CB[7] has thus been isolated by this method, and many of them have been applied in a biomedical context. In particular, a monoazido-CB[7] also appeared to be a key compound to access many derivatives by click chemistry with relevant monopropargyl derivatives. However, and as for the other methods, CB[8] remains reluctant to functionalization even if a few derivatives are known[57,58] and despite the enormous interest in accessing such derivatives owing to the larger cavity of this CB member.

3. APPLICATIONS OF *F*-CB[5]

The smallest member of the cucurbituril family, CB[5], is featured by a small cavity, making the scope of molecules to include narrow despite showing the highest solubility in the series.[10] The modest size of the CB[5] cavity is suitable to include several gas molecules, such as N_2, O_2, Ar, NO, or CO_2 as documented for decamethyl-CB[5] (**CB[5]-(Me)$_{10}$**) in the solid state.[59] Later, Huber and co-workers showed that perhydroxylated-CB[5] (**CB[5]-(OH)$_{10}$**, Figure 2) could bind O_2

Figure 2. Chemical structure of **CB[5]-(OH)$_{10}$** (the hydroxyl groups enhance the ability to bind oxygen molecules).

at 37 °C and in the presence of NaCl at a concentration relevant in blood (but not **CB[5]-(Me)$_{10}$**).[60] Even if toxicology studies are required to confirm the relevance of **CB[5]-(OH)$_{10}$** to transport oxygen in biological media, these results are promising enough to envision its use as a substitute to hemoglobin.

4. APPLICATIONS OF *F*-CB[6]

With a larger cavity compared to that of CB[5], CB[6] can bind aliphatic guest molecules, often positively charged, with large binding constants.[61] This enabled investigation of a larger set of compounds to be included in CB[6], but difficulties in its functionalization (low solubility) and possible low solubility in water even after modifications are likely to have hampered developments in this direction as can be checked by the small number of *F*-CB[6] reported. Another reason may stand in the still quite restricted number of includable guest molecules as compared to those possible with CB[7] or CB[8]. Nevertheless, a few examples have been described using monofunctionalized CB[6], and more studies have been devoted to perfunctionalized CB[6], polymerized to produce macrocyclic vesicles for various usages.

4.1. *F*-CB[6] in Therapy and Bioimaging

After the successful synthesis and isolation of perallyloxy-CB[6] (**CB[6]-(O-allyl)$_{12}$**, Figure 3),[41] Kim and co-workers

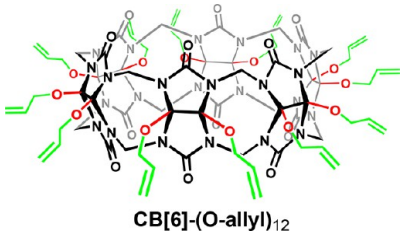

Figure 3. Chemical structure of **CB[6]-(O-allyl)$_{12}$** (the alkene groups allow further functionalization and polymerization).

further functionalized it by thiol−ene click chemistry with small PEG chains and prepared a **CB[6]-(PEG$_3$)$_{12}$** derivative using 2-[2-(2-methoxyethoxy)-ethoxy]-ethanethiol.[62]

Next, they could trigger the self-assembly of **CB[6]-(PEG$_3$)$_{12}$** into supramolecular vesicles featured by diameters from ∼30 to 1000 nm and a membrane thickness of ∼6 nm. The surface of the vesicles was featured by the abundant presence of CB[6] cavities, making it easily amenable to further modification by host−guest chemistry. After having anchored mannose derivatives on the vesicles, via conjugation to spermidine (included in the surface CB[6] cavities), the sugar-decorated vesicles could recognize concanavalin A with a high affinity. Next, Kim and co-workers replaced monothiols by dithiols to cross-link **CB[6]-(O-allyl)$_{12}$** and prepare covalent *F*-CB[6] polymer nanocapsules.[63,64] This strategy set the foundation for several studies in the biomedical context. The covalent *F*-CB[6] nanocapsules were featured by an average diameter of ∼100 nm and a shell thickness of ∼2.1 nm. However, 2D oligomeric objects were observed to form rolled or folded objects rather than nanocapsules in DMF. Based on this discovery, this team further developed a method to produce free-standing *F*-CB[6]-based 2D polymers with single-monomer thickness.[65] To enable the discovered *F*-CB[6] nanocapsules to respond to a relevant stimulus, Kim and co-workers next prepared new nanocapsules by grafting amino groups at the periphery of CB[6] (**CB[6]-(NH$_2$)$_{12}$**) before cross-linking with disulfide linkers.[66]

The on-surface CB[6] provided easy noncovalent (albeit robust) functionalization for HepG2 cell internalization by receptor-mediated endocytosis, the capsule internal space, room for encapsulating model cargo molecules, and the linker's in-cell responsiveness to reduction for capsule degradation and cargo release. Subsequently, the same group developed a modular bioimaging platform based on *F*-CB[6] nanocapsules to realize multimodal cancer-targeted in vivo imaging (Figure 4a).[67] The high binding affinity between CB[6] and

https://doi.org/10.1021/jacsau.3c00273
JACS Au 2023, 3, 2356−2377

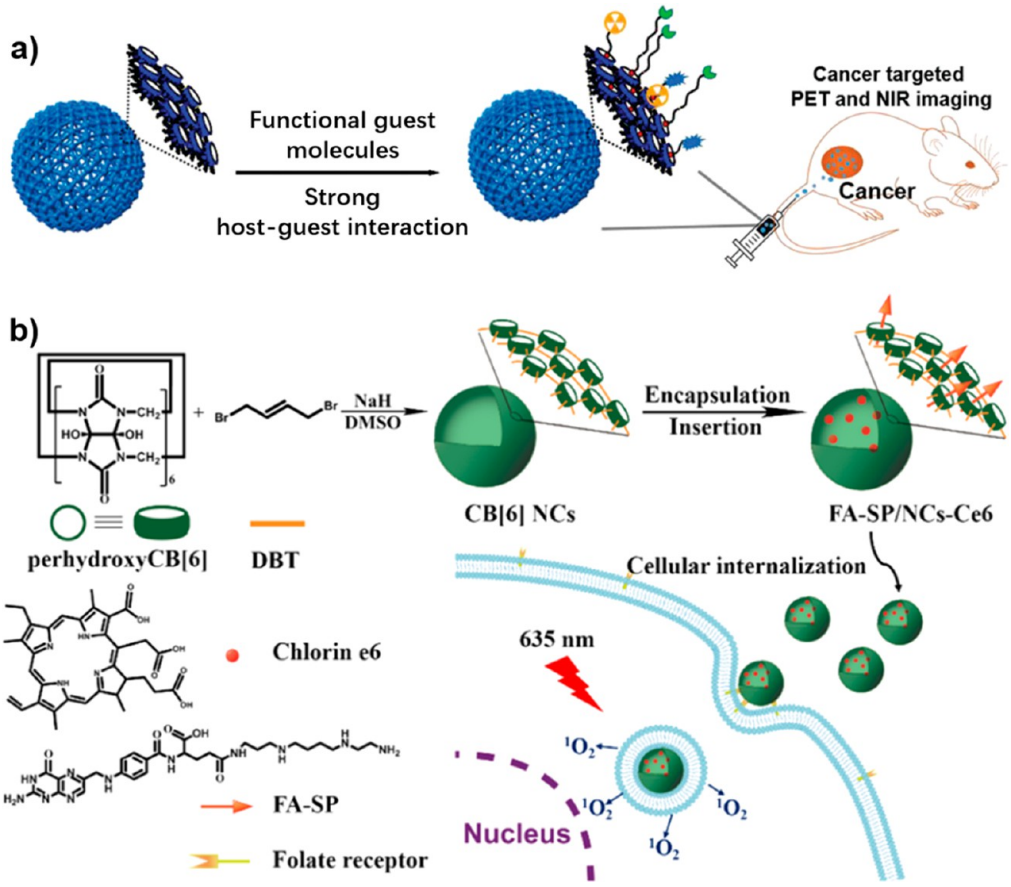

Figure 4. a) Facile surface modification of *F*-CB[6] nanocapscule and the use of CB[6]-based nanocapsule as a robust and multifunctional platform for multimodal imaging of a cancer-bearing mouse. Reprinted with permission from ref 67. Copyright 2017 Royal Society of Chemistry. b) Schematic illustration of preparation of *F*-CB[6]-based nanocapsules for targeted delivery and PDT. Reprinted with permission from ref 68. Copyright 2019 American Chemical Society.

spermidine (spmd) in vivo was used to prepare three new molecules: a cyanine 7, a ^{64}Cu-NOTA complex, and a cyclic RGDyK peptide, all modified with spmd and inserted on the surface of the nanocapsules by CB[6] complexation. This strategy allowed an efficient combination of in vivo cancer targeting and visualization by near-infrared (NIR) imaging and positron emission tomography (PET) in mice.

The usefulness of *F*-CB[6] nanocapsules was clearly demonstrated in previous examples. However, difficulties in obtaining **CB[6]-(O-allyl)$_{12}$** incited researchers to find an alternative way to produce *F*-CB[6] nanocapsules. Wang and co-workers thus developed a more direct method to get analogous nanocapsules from perhydroxy-CB[6] using double alkylation by a ditopic linker.[68] Chlorin e6 (Ce6) was next successfully loaded in the new *F*-CB[6] nanocapsules before surface decoration by folic acid−spermine (FA-SP) conjugates for targeted cellular delivery. The new *F*-CB[6]-based nanocapsule showed good photodynamic therapy (PDT) activity in vitro (Figure 4b). Subsequently, Wang and co-workers introduced an azobenzene unit (AZO) in the linker between perhydroxy CB[6] macrocycles to study the possibility for cargo release by light.[69,70] Two different mechanisms were proposed whether the system was applied in vitro or in vivo, relying either on (i) light-induced *trans*−*cis* isomerization of the azo bond or (ii) hypoxia-induced breakdown of the azo bond, illustrating their potential in drug controlled release.

4.2. *F*-CB[6]s in Tissue Engineering

Tissue engineering is a developing modern clinical application.[71] Kim and co-workers developed engineered supramolecular hydrogels mimicking the 3D organization of live tissue using a complex of (i) a CB[6] conjugate of hyaluronic acid (HA): **CB[6]-HA** (Figure 5), (ii) a diaminohexane conjugate of HA (DAH-HA), and (iii) a CB[6] conjugate of

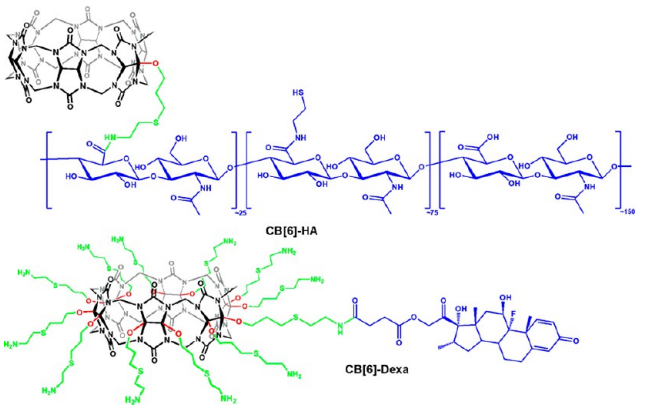

Figure 5. Chemical structures of **CB[6]-HA** (the functional group was modified for the construction of hydrogel) and **CB[6]-Dexa** (the functional group is a synthetic glucocorticoid to induce the differentiation of MSCs to chondrocytes).

https://doi.org/10.1021/jacsau.3c00273
JACS Au 2023, 3, 2356−2377

dexamethasone (**CB[6]-Dexa**, Figure 5).[72] This combination was used for the controlled chondrogenesis of human mesenchymal stem cells (hMSCs). The *F*-CB[6]-based supramolecular hydrogels could act as good scaffolds for cartilage regeneration via controlled drug delivery. Although less developed than other applications, this work demonstrated the relevance of using *F*-CB[6] for tissue engineering and aims to foster more work in this direction.

4.3. *F*-CB[6]s in Sensor Devices

Sensors are key devices regularly used in our everyday life. In particular, organic field-effect transistor (OFET)-based sensors possess several advantages like simple fabrication, low cost, versatile usages, and high sensitivity.[73] Acetylcholine (ACh^+), an important neurotransmitter of the human central nervous system, and choline (Ch^+), a smaller analogue of ACh^+, are involved in several biological functions. Detecting and quantifying their presence are currently needed, but traditional methods based on acetylcholine esterase (AChE) have low detection limits (μM to nM). Kim and co-workers have developed a perallyoxy-CB[6]-based OFET for the selective detection of ACh^+ over Ch^+, with a low detection limit of 1×10^{-12} M (pM).[73] Compared with unmodified CB[6] featured by low solubility and so low processability, perallyoxy-CB[6] showed higher binding affinity and selectivity toward ACh^+, and its good solubility in alcohol enabled easy device fabrication by spin coating.

5. APPLICATIONS OF *F*-CB[7]

With a relatively large cavity binding aliphatic groups as well as aromatic compounds,[10] CB[7] has attracted the most attention from the supramolecular community. With a relatively good solubility in water and just about sufficient in DMSO, several dozens of CB[7] derivatives have been obtained and used in the biomedical context. Hence, the growing field of *F*-CB[7] has passed from a burgeoning area to a flourishing domain with several categories of functional groups appended to CB[7] like targeting groups, anchoring groups, fluorescent groups, or informed (DNA) groups, all used for various biomedical applications.

5.1. Targeting CB[7] to Reach Specific Cells or Tissues

CB[7] has shown interesting potential for drug solubilization and stabilization by sequestration followed by passive release toward a wide range of bioactive molecules.[14] However, in most cases, CB[7] is used in vitro,[74,75] since it cannot distribute very specifically in vivo. To overcome this limitation, Isaacs, Briken, and co-workers reported in 2013 the first targeting cucurbiturils: two biotin-functionalized CB[7]s (**CB[7]-biotins**, Figure 6) for the targeted delivery of oxaliplatin to cancer cells.[76] As anticipated, the presence of biotin significantly enhanced the efficiency of CB[7]-biotin to target biotin receptors and deliver the loaded drugs at relevant sites, resulting in improved drug efficacy. In this paper, Isaacs and co-workers also described the synthesis of the first CB[7] peptide conjugates, namely **CB[7]-glutathione** and **CB[7]-cyclo-(Arg-Gly-Asp-D-Phe-Cys)**, although they did not report on biological applications with these compounds.

In 2018, Agasti and co-workers reported the synthesis and use of CB[7]-conjugated antibodies **CB[7]-Ab** targeting microtubules in fixed mouse embryonic fibroblast (MEF) cells,[77] before capitalizing on the tight binding of CB[7] for adamantane derivatives to fluorescently label the microtubules by an adamantane-functionalized Cy5 fluorescent dye.

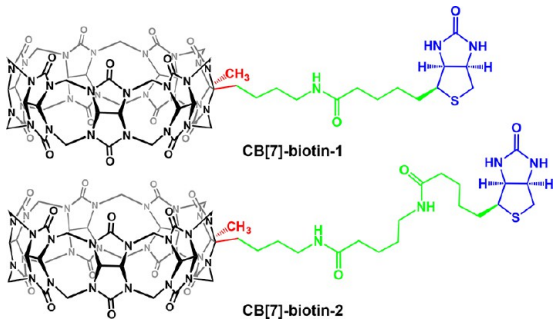

Figure 6. Chemical structures of different **CB[7]-biotins** (the biotin-based functional group was introduced for improving targeting efficiency).

Remarkably, the fluorescent staining, which was stable after multiple washing steps, was highly specific to the microtubules. This was next used to perform super-resolution imaging of the microtubule network by a combination of an adamantane-functionalized DNA strand, complementary to another strand carrying a new-generation fluorescent dye for cell imaging. In the same paper, a **CB[7]-Phalloidin** (Figure 7) conjugate was

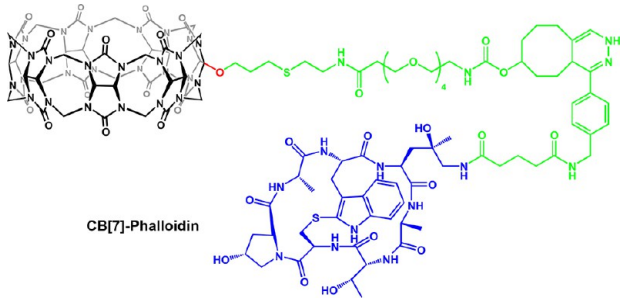

Figure 7. Chemical structure of **CB[7]-Phalloidin** (the functional group was introduced for targeting F-actin).

prepared for F-actin targeting. Phalloidin is a bicyclic heptapeptide known for its high level of specific binding for F-actin. Using this new targeting CB[7], the authors specifically labeled the actin cytoskeleton of ovary tissues of *Drosophila melanogaster* before fluorescence imaging by coincubation with an adamantane-functionalized Cy5. The authors conclude with live-cell biorthogonal multiplex imaging using **CB[7]-Abs** specifically targeting mitochondria, microtubules, and actin and relevant conjugated fluorescent dyes.

In 2021, Houghton and co-workers reported an anticarcinoembryonic antigen antibody modified CB[7]: **CB[7]-M5A**.[78] This conjugate was used combined with a ^{68}Ga-radiolabeled ferrocene guest radioligand as a pretargeting agent for positron emission tomography in BxPC3 xenografted nude mice. The targeting CB[7] enabled improved tumor uptake of the radioligand. This approach was further explored in 2022[79] using the same **CB[7]-M5A** but this time combined with other radioligands: [^{64}Cu]Cu-NOTA-PEG$_3$-Fc and [^{64}Cu]Cu-NOTA-PEG$_7$-Fc) benefiting again of the ultrahigh binding of the appended ferrocene moiety (Fc) of the radioligands toward CB[7]. Results showed specific tumor uptake with excellent extended lag time, suggesting possible use without clearing agents that have until now complicated clinical applications of this technique.

In 2023, Lecorche, Jacquot, Bardelang, and co-workers reported the synthesis of a peptide-targeting CB[7], **CB[7]-**

https://doi.org/10.1021/jacsau.3c00273
JACS Au 2023, 3, 2356−2377

VH4127 (Figure 8), enabling cell uptake by receptor-mediated transport through specific and noncompetitive Low Density Lipoprotein (LDL) receptor (LDLR) binding (Figure 9).[80] Cell uptake and trafficking could be followed using an adamantane-functionalized Alexa680 fluorescent conjugate (**A680-ADA**), again benefiting from the ultrahigh binding of adamantane derivatives toward CB[7]. Results showed that the **A680-ADA•CB[7]-VH4127** complex was stable over HPLC purification and in cells and showed better endocytosis potential compared with the direct A680-VH4127 conjugate. With LDLR being overexpressed in several tumor types, this conjugate could be a relevant targeting cargo for addressing anticancer drugs specifically, thereby reducing side effects and improving therapeutic efficacy.[80]

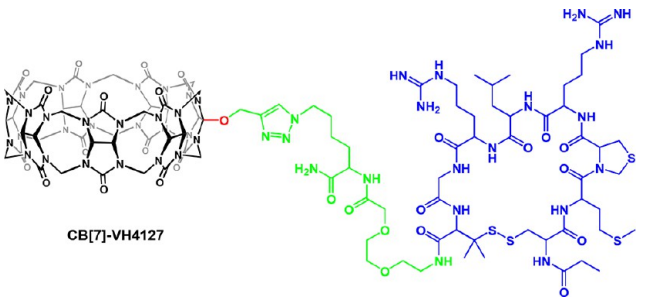

Figure 8. Chemical structure of **CB[7]-VH4127** (the functional group offers the ability to target LDLR to enhance cell uptake).

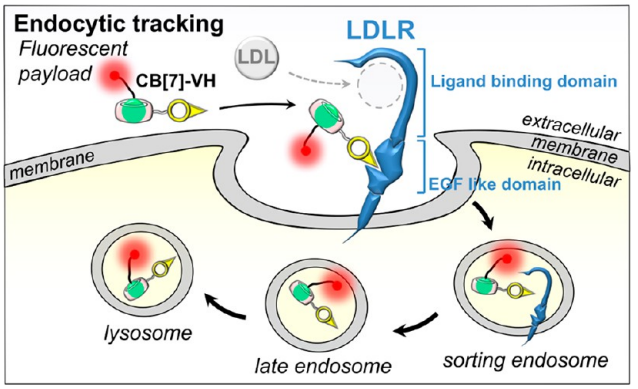

Figure 9. **CB[7]-VH4127** conjugate targeting LDLR for efficient intracellular delivery in LDLR expressing cells. Reprinted with permission from ref 80. Copyright 2023 American Chemical Society.

5.2. *F*-CB[7]s in Molecular and Cell Biology

In 2011, Kim and co-workers developed an *F*-CB[7]-based supramolecular latching system for applications in proteomics.[81] They have employed CB[7] decorated beads (**CB[7]-beads**, prepared from **CB[7]-OH**) to bind 1-trimethylammoniomethylferrocene (AFc)-conjugated proteins to collect and enrich plasma membrane proteins.[82] Subsequently, they extended their technique to the intracellular proteome.[83] **CB[7]-beads** were used to bind suberanilohydroxamic acid−ammonium-adamantane (SAHA-Ad)-labeled histone deacetylases from an MDA-MB-231 breast cancer cell lysate to realize the enrichment of intracellular proteins. This method showed several advantages compared to classical methods involving click chemistry and biotin−streptavidin, such as better water solubility and higher yields. Next, the supramolecular latching system by **CB7-beads** was employed to purify recombinant proteins (Figure 10), including Herceptin and cytokine interferon α-2a, avoiding issues like contamination, protein denaturation, and critical conditions for protein capture.[84] Then, they proceeded to protein tagging (plasma membrane, intracellular/organelle proteins, and a mutant of the DNA-repair protein) by adamantane derivatives before protein imaging using CB[7] conjugated to cyanine fluorescent dyes.[51]

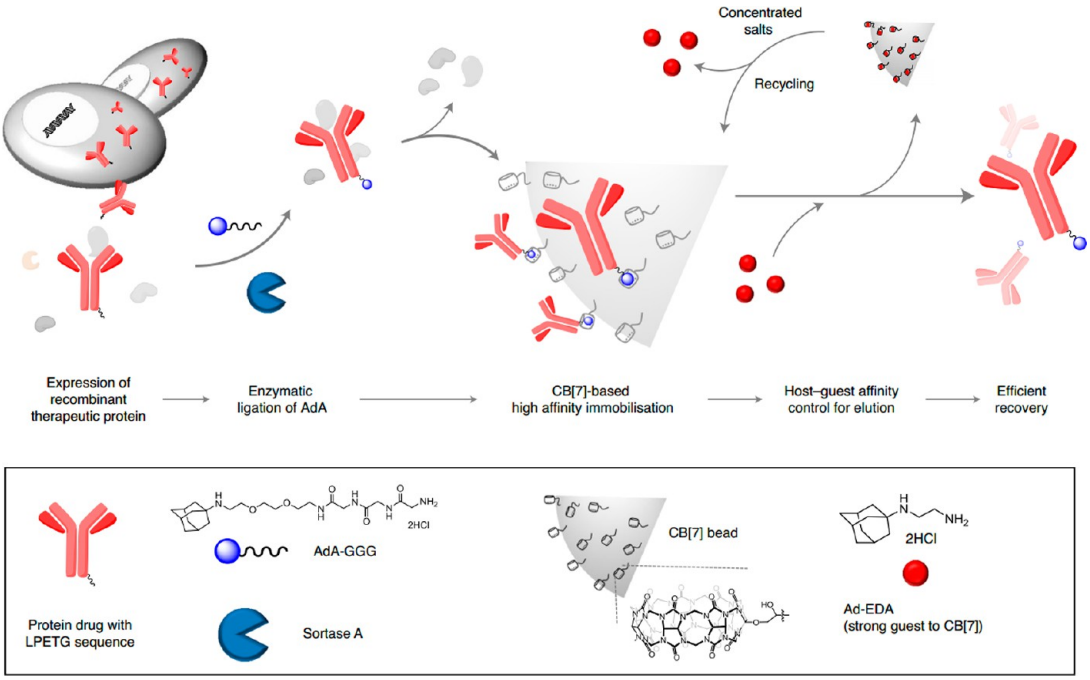

Figure 10. **CB[7]beads**-based affinity chromatography for the purification of therapeutic proteins. Reprinted with permission from ref 84. Copyright 2020 Springer Nature.

https://doi.org/10.1021/jacsau.3c00273
JACS Au 2023, 3, 2356−2377

The cyanine 3-conjugated CB[7] (**CB[7]-Cy3**, Figure 11) was used to bind the tagged proteins, thus allowing for precise

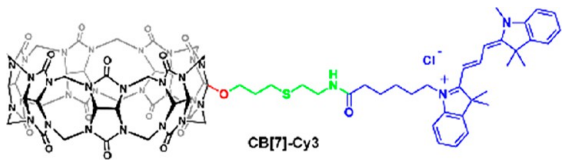

Figure 11. Chemical structure of **CB[7]-Cy3** (the functional group was introduced as a fluorescent tracer).

analyses of proteins located in and on fixed living cells by fluorescence imaging. Next, they used **ADA-COOH** to modify the proteins on the surface of *C. elegans* (a roundworm). After addition of **CB[7]-Cy3**, a red fluorescence appeared on its surface, indicating that the visualization of proteins on live animals is possible with this technique.[51] Thereafter, Kim and co-workers used the pair **CB[7]-Cy3** with **ADA-BDP630/650** (adamantane conjugate of boron-dipyrromethene 630/650X) to confirm the binding of ADA and CB[7] inside *C. elegans* by fluorescence resonance energy transfer (FRET).[85] Then, they conjugated Erbitux, an antibody targeting the human epidermal growth factor receptor for the treatment of neck, colorectal, and lung cancers, to CB[7] (**CB[7]-Erbitux**).[85] After binding of **CB[7]-Erbitux** to cancer cells, a following injection of **ADA-Cy5** could target **CB[7]-Erbitux**-bound cancer cells and achieve bio-orthogonal in vivo cancer imaging.

Besides, Kim and co-workers developed a single-vesicle content-mixing assay based on tight CB[7] binding, and FRET between **CB[7]-Cy3** and **ADA-Cy5**, where Cy3 and Cy5 act as donor dye and acceptor dye, respectively.[86] The **CB[7]-Cy3** and **ADA-Cy5** conjugates were encapsulated in different vesicles, and the flickering fusion could be monitored in vitro by the strong FRET effect after binding between **CB[7]-Cy3** and **ADA-Cy5** (Figure 12).

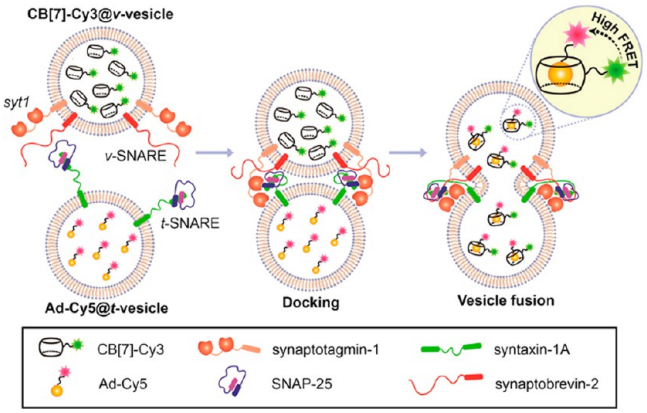

Figure 12. Schematic illustration of SNARE-mediated content mixing using a host–guest FRET pair. Reprinted with permission from ref 86. Copyright 2015 American Chemical Society.

The same method was subsequently exploited to study autophagy. **CB[7]-Cy3** was intracellularly translocated in lysosomes, while **ADA-Cy5** was accumulated in mitochondria. After the fusion of lysosomes and mitochondria, the FRET signal appeared as a result of the host–guest interaction between **CB[7]-Cy3** and **ADA-Cy5**, successfully visualizing the autophagosome–lysosome fusion process.[87]

Seitz and co-workers employed DNA to explore the limits of bivalency using CB[7]•ADA binding pairs and DNA to control the distance (70–360 Å) between the CB[7] and adamantane groups (**CB[7]-DNA-1-1**, **CB[7]-DNA-1-2** and **CB[7]-DNA-1-3**, Figure 13).[88] The results showed that the

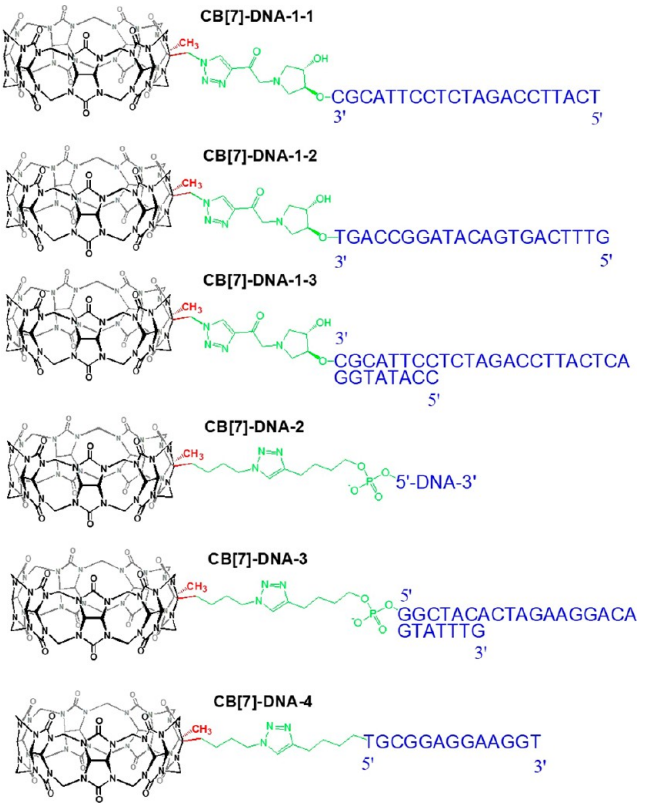

Figure 13. Chemical structures of different **CB[7]-DNAs** modified with various DNA fragments. (The functional groups can enhance the specific binding properties according to the principle of complementary base pairing).

distance between the two recognition modules, scaffold flexibility, and binding affinity of each recognition module can influence the binding properties of a bivalent system. In another context, Mao and co-workers used DNA and optical tweezers to determine the mechanical features of the host–guest interaction between CB[7] and ADA (**CB[7]-DNA-2** and **CB[7]-DNA-3**, Figure 13).[89] The forces maintaining CB[7] on positively charged ADA and neutral ADA were determined to be 49 and 44 pN, respectively.

Besides, Isaacs and co-workers modified CB[7] (**CB[7]-DNA-4**, Figure 13) and ADA (**ADA-DNA**) by single-strand DNA, forming a duplex in the presence of adenosine triphosphate (ATP).[90] A protein inhibitor was initially located in the cavity of **CB[7]-DNA-4**, then released after ATP triggered duplex formation (Figure 14).

Finally, Jayawickramarajah and co-workers used the CB[7]•ADA host–guest pair as a surrogate to replace the regularly used base pair for DNA strand displacement, modulating enzyme activity and layered reactions detecting specific microRNA.[91] This method is a positive alternative to the traditional base-pair-driven, toehold-mediated strand displacement, enhancing the diversity of the toolbox for the manipulation of the function of dynamic DNA machines.

https://doi.org/10.1021/jacsau.3c00273
JACS Au 2023, 3, 2356–2377

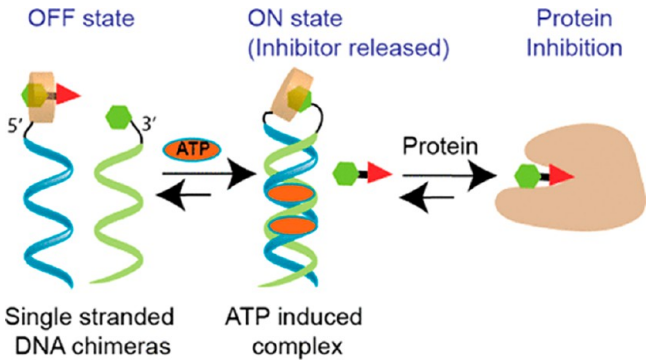

Figure 14. Schematic illustration of ATP-fueled release of the protein inhibitor. Reprinted with permission from ref 90. Copyright 2017 American Chemical Society.

Recently, Wang and co-workers employed supramolecular systems based on hyaluronic acid (HA)-modified CB[7] (**CB**[7]-**HA**, Figure 15) and TPP-PEG-ADA (TPP: triphenyl-

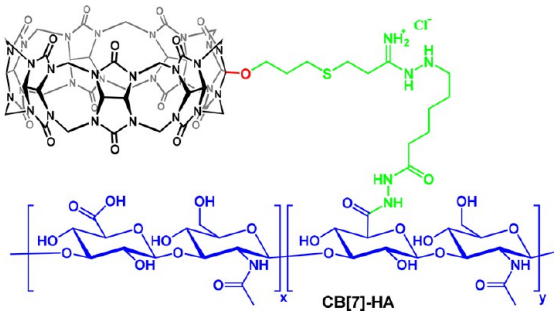

Figure 15. Chemical structure of **CB**[7]-**HA** (the functional group was introduced as scaffold for mitochondrial aggregation and fusion).

phosphonium, a well-known moiety targeting mitochondria)[92] to get some control on the biological properties of mitochondria (Figure 16).[52] By mixing TPP-PEG-ADA with

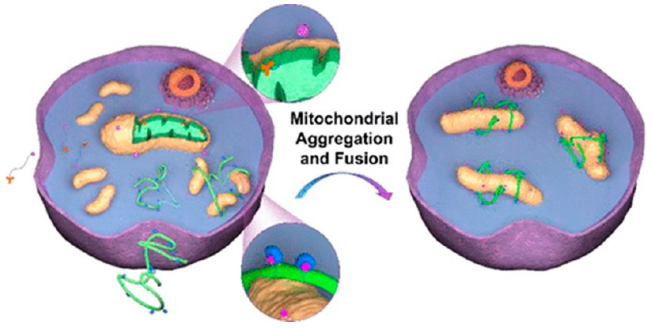

Figure 16. Schematic illustration of supramolecular mitochondrial aggregation and fusion. Reprinted with permission from ref 52. Copyright 2020 American Chemical Society.

mitochondria, the latter were decorated with many ADA groups, tightly recognizing CB[7]. By adding **CB**[7]-**HA**, the CB[7]•ADA recognition triggered the aggregation and fusion of mitochondria, alleviating possible adverse damages induced by mitochondrial fission, which could be confirmed both in vitro and in vivo.

5.3. *F*-CB[7]s in Bioimaging and Therapy

Fluorescent cucurbit[7]uil (**CB**[7]-**Cy3**) has already been mentioned and used for several biological applications.[51,86,87] As unmodified CB[7] is not fluorescent, conjugation with a relevant chromophore is needed if fluorescent tracking is envisioned. For instance, Urbach and co-workers have conjugated CB[7] to tetramethylrhodamine (TMR, **CB**[7]-**TMR**, Figure 17).[93] Confocal fluorescence microscopy showed

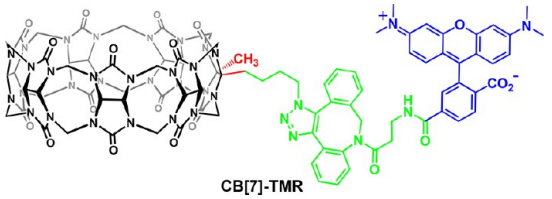

Figure 17. Chemical structure of **CB**[7]-**TMR** (the dye-based functional group was introduced as a fluorescent tracer).

CB[7]-**TMR** uptake in live neurons and its corresponding location in the cytoplasm (Figure 18), possibly by endocytosis.

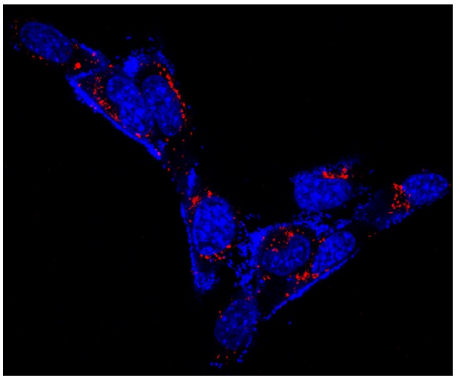

Figure 18. False color confocal fluorescence micrograph of live HT22 cells treated with 91 μM **CB**[7]-**TMR** (red) and Hoechst 33342 (blue). Reprinted with permission from ref 93. Copyright 2020 American Chemical Society.

The authors also showed that the fluorescence of the conjugate was quenched upon guest binding and that guest affinity for the host was essentially unchanged.

Almost at the same time, Isaacs and co-workers conjugated CB[7] to poly(ethylene glycol) (PEG, **CB**[7]-**PEG**, Figure 19), the conjugate binding several proteins and thereby increasing their stability and biopharmaceutical activity (Figure 20).[94]

Beside covalent protein conjugation, this supramolecular kind of modification opened the way to adding prosthetic functionality to proteins by simple mixing with a relevant *F*-

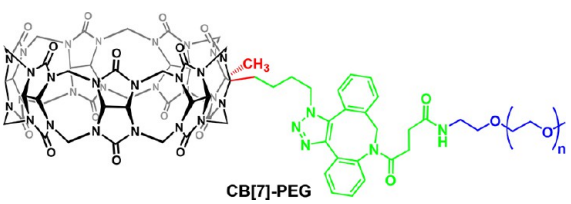

Figure 19. Chemical structure of **CB**[7]-**PEG** (the PEG-based functional group was introduced to enhance biocompatibility).

https://doi.org/10.1021/jacsau.3c00273
JACS Au 2023, 3, 2356−2377

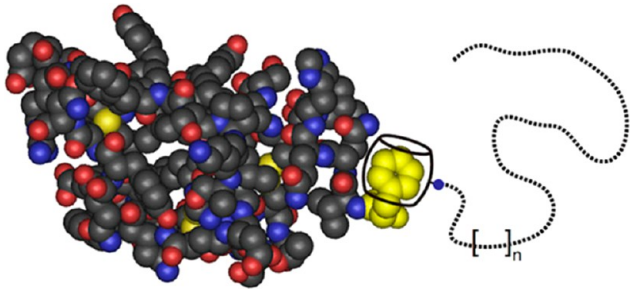

Figure 20. Cartoon depicting supramolecular PEGylation of the insulin protein through strong noncovalent binding of the CB[7] moiety to the *N*-terminal phenylalanine residue. Reprinted with permission from ref 94. Copyright 2016 National Academy of Science.

CB[7]. Indeed, leveraging the established strong host−guest interaction between CB[7] and *N*-terminal aromatic amino acids,[13] three different proteins were tested (glucagon, Rituximab, and insulin), with the addition of **CB[7]-PEG** resulting in better solubilities and inhibition of protein aggregation. In vivo tests on mice showed a prolonged activity of insulin after supramolecular modification by **CB[7]-PEG**, in part ascribed to the additional molecular weight impacting lymphatic absorption rates.[95] Subsequently, **CB[7]-PEG** was used to enhance the therapeutic efficacy of a coformulation of insulin and pramlintide.[96] Indeed, the coadministration of insulin with pramlintide is more effective than insulin alone, but the mixture is unstable, requiring the two compounds to be administrated separately. After supramolecular pegylation by **CB[7]-PEG**, the coformulation could be stabilized for over 100 h at 37 °C under continuous stirring, improving the stability time of insulin commercial formulations (aggregation after 10 h). Furthermore, **CB[7]-PEG** also improved the pharmacokinetics of insulin and pramlintide and increased postprandial glucagon suppression in diabetic pigs, showing the potential application for dual-hormone replacement therapy.

In parallel, Zhang and co-workers prepared a CB[7]-based polymer with PEG chains (**poly-CB[7]**) for drug delivery and anticancer therapy (Figure 21).[97] Bis-alkyne functionalized CB[7] was synthesized by direct functionalization and linked by PEG to integrate CB[7] in the main chain of the polymer. Compared to unmodified CB[7],[75] **Poly-CB[7]** loaded with oxaliplatin showed enhanced anticancer activity both in vitro

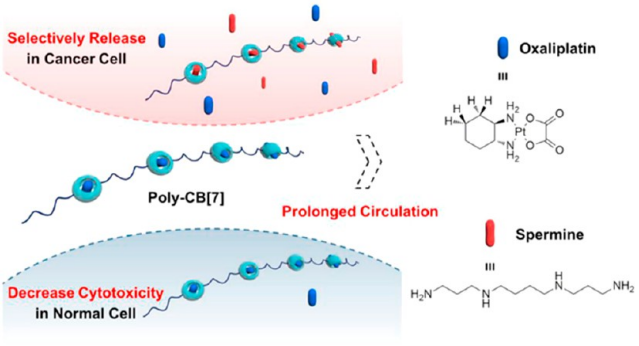

Figure 21. Schematic illustration of supramolecular polymeric chemotherapy based on **poly-CB[7]**. Reprinted with permission from ref 97. Copyright 2018 Elsevier.

(HCT116, colorectal cancer cell line) and in vivo, as well as longer circulation performance in vivo due to the presence of PEG fragments.

Nanomedicine is one of the most active research fields for biomedical applications.[98] In this context, Isaacs and co-workers used metal−organic polyhedra to assemble **CB[7]-bis(pyridine)** (Figure 22) into CB[7]-decorated nanoparticles

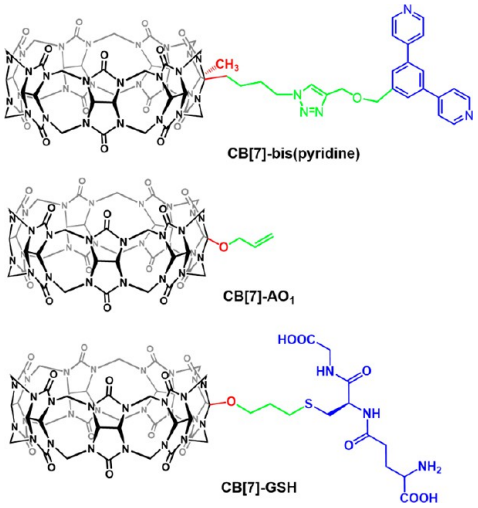

Figure 22. Chemical structures of **CB[7]-bis(pyridine)** (the functional group was introduced to construct MOP), **CB[7]-AO$_1$** (the functional group offers the function of surfactant in water), and **CB[7]-GSH** (the functional group was modified to interrupt nano vesicles for drug delivery).

for drug delivery (Figure 23A).[99] The Fujita-type MOP assembled by palladium ions and bis-pyridines[100,101] served as a nanoparticle scaffold to (i) host Nile Red (NR) or Doxorubicine (DOX) and (ii) carry on dangling CB[7] rings used to enable the inclusion of guest molecules in MOP by the hydrophobic effect, and their release upon competitive binding in the appended CB[7]. This **CB[7]-MOP** approach was then translated successfully in vitro using HeLa cells.

Subsequently, Kim and co-workers demonstrated the possibility to use monoallyloxy-CB[7] (**CB[7]-AO$_1$**, Figure 22) as a building unit for the construction of nano vesicles (Figure 23B).[46] They discovered that **CB[7]-AO$_1$** behaved as a nonclassical surfactant in water, self-assembling in responsive nano vesicles. Although the mechanism is not fully understood, the presence of the monoallyloxy group is postulated to be the origin of this peculiar behavior. Then, they introduced glutathione (GSH) as a guest to be bound in the cavities of **CB[7]-AO$_1$** vesicles. After light irradiation, GSH was conjugated to **CB[7]-AO$_1$** to form **CB[7]-GSH** (Figure 22) by means of thiol−ene click chemistry, disrupting the morphology of the vesicles and releasing previously loaded cargos. **CB[7]-AO$_1$** vesicles loaded with doxorubicine showed good light-triggered drug release in vitro, as tested on HeLa cells.

Thereafter, Wang and co-workers constructed surface programmable nanoparticles based on poly(lactic acid) (PLA)-modified CB[7] (**CB[7]-PLA**, Figure 24) and poly-(lactic-*co*-glycolic acid) (PLGA) for drug delivery.[102] The abundant CB[7] cavities exposed on the surface of the drug-loaded nanoparticles allowed further easy modifications by inserting molecules with different structures, imparting addi-

https://doi.org/10.1021/jacsau.3c00273
JACS Au 2023, 3, 2356−2377

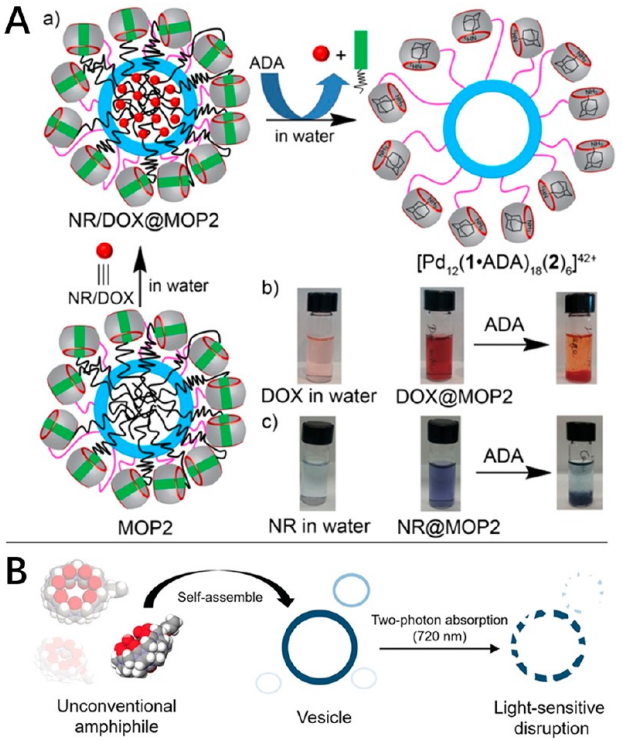

Figure 23. (A) Schematic representation (a) of the chemically responsive release of NR or DOX from the hydrophobic cavity of MOP2 by ADA. (b and c) Naked eye detection of hydrophobic guest encapsulation and chemical-responsive release (b, DOX; c, NR). Reprinted with permission from ref 99. Copyright 2017 American Chemical Society. (B) Schematic illustration of monoallyloxy CB[7] for the construction of light responsive nano vesicles. Reprinted with permission from ref 46. Copyright 2018 John Wiley and Sons.

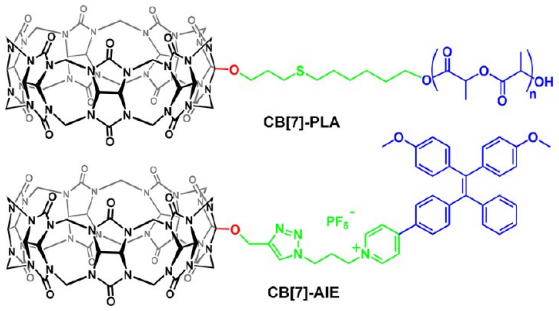

Figure 24. Chemical structures of **CB[7]-PLA** (the functional group was introduced to construct nanoparticles) and **CB[7]-AIE** (the functional group was introduced as a fluorescent indicator).

tional functions like targeting, fluorescence, and secondary drug binding. Following a similar approach consisting of incorporating *F*-CB[7] in (or assembling *F*-CB[7] as) nanoparticles, these systems were used for (i) responsive drug delivery,[103] (ii) combined photodynamic therapy (PDT) and chemotherapy (**CB[7]-AIE**, Figure 24 and 25),[104] and (iii) deep-tissue-inflammation imaging.[105]

The fusion of organic and inorganic structures can combine the advantages of both worlds, as perfectly illustrated by the **CB[7]-MOP** developed by Isaacs.[99] This kind of hybrid materials has shown great performance in biomedical applications.[106] For instance, Wang and co-workers have prepared and studied hybrid materials made of *F*-CB[7] and gold nanorods,[107,108] iron nanoparticles,[109,110] and graphene.[111] Compared with CB[7]-decorated organic materials,[112] the presence of metals in CB[7]-decorated metallic materials imparted new features in these hybrid materials. Au nanorods have started to be used as bioactive agents in photothermal therapy (PTT), due to their absorption in the NIR spectrum and ability to transform the collected energy into heat. The modification of the surface of Au nanorods by **CB[7]-NH$_2$** (Figure 26) enabled the addition of several new features, including targeting and drug transportation, thanks to the numerous appended CB[7].

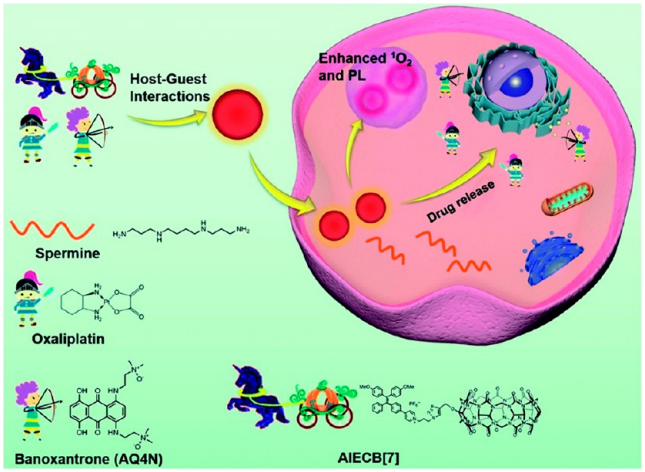

Figure 25. Schematic illustration of the use of **CB[7]-AIE** for imaging-guided, synergistic PDT and supramolecular chemotherapy. Reprinted with permission from ref 104. Copyright 2021 Royal Society of Chemistry.

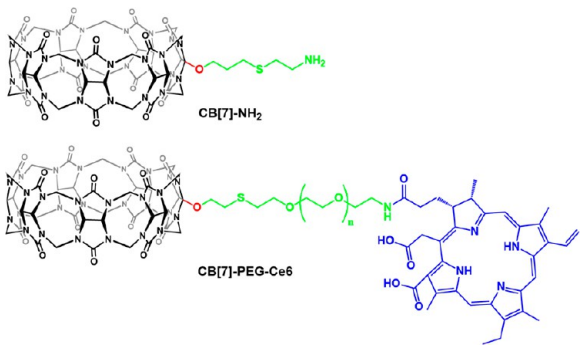

Figure 26. Chemical structures of **CB[7]-NH$_2$** (the functional group was introduced to connect Au nanorods) and **CB[7]-PEG-Ce6** (the functional group was introduced for the function of PDT).

The **CB[7]-Au nanorods** demonstrated improved therapeutic activity due to the synergistic combination of chemotherapy and photothermal therapy (Figure 27).[107] The combination of **CB[7]-Au nanorods** with protein-70 promoter-based plasmid (Hsp-plasmid) formed supramolecular vesicles, which were next used simultaneously for PTT and gene delivery. This strategy showed improved overall therapeutic efficacy against tumors in both in vitro and in vivo assays.[108]

In parallel, the surface of Fe_3O_4 nanoparticles, known for magnetic field guided targeting and magnetic resonance imaging, was modified to carry on CB[7], preventing nanoparticle aggregation in water and offering additional cavities to accommodate drug molecules and targeting units.[109]

https://doi.org/10.1021/jacsau.3c00273
JACS Au 2023, 3, 2356−2377

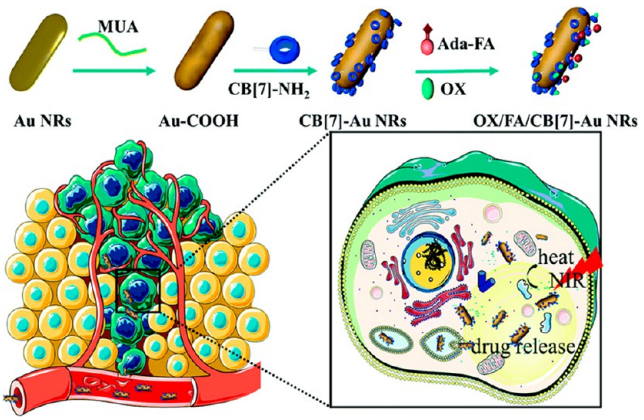

Figure 27. Schematic diagram showing the preparation of the OX/FA/**CB**[7]-**Au nanorods** and the principles of synergistic chemo-photothermal therapy. Reprinted with permission from ref 107. Copyright 2019 Royal Society of Chemistry.

Later, **CB**[7]-**Fe_3O_4 nanoparticles** were used as guided artificial receptors in a stepwise injection protocol, to accommodate subsequent therapeutic agents.[110] After magnetic accumulation of **CB**[7]-**Fe_3O_4 nanoparticles** in a tumor, Ferrocene (Fc)-modified Au nanoparticles (**Fc-Au nanorods**) focused around the CB[7]-modified magnetic nanoparticles in the tumor via strong binding between CB[7] and Fc, thereby realizing stepwise targeting PTT.

Besides metallic particles, nano graphene oxide (NGO) is another popular compound used to build hybrid materials. The simultaneous use of Ce6 and *F*-CB[7] (**CB**[7]-**PEG-Ce6**, Figure 26) proved to be a good combination of PDT and chemotherapy.[113] To develop multimodal treatments, the addition of NGO to Ce6 and *F*-CB[7] enabled the construction of a multifunctional supramolecular system for an efficient cancer therapy combining PTT, PDT, and dual chemotherapy using oxaliplatin and banoxantrone (Figure 28).[111]

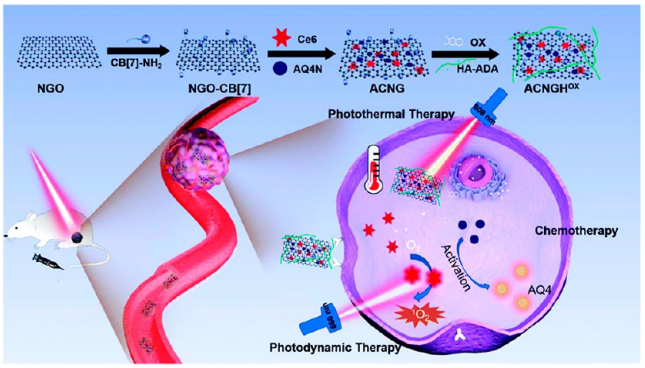

Figure 28. Preparation of **CB**[7]-**NGO** for photothermal/photodynamic and hypoxia-activated chemotherapy of cancer. Reprinted with permission from ref 111. Copyright 2021 Royal Society of Chemistry.

Beside traditional drug delivery methods, new methods based on *F*-CB[7] have emerged.[114,115] Webber and coworkers prepared micelles using F127 linked CB[7] dimers (**CB**[7]-**F127-CB**[7]) and complementary **Fc-PEG_8** units to offer an artificial host for the following drug delivery (Figure 29).[114] The mixture of **CB**[7]-**F127-CB**[7] and PEG_8-Fc can

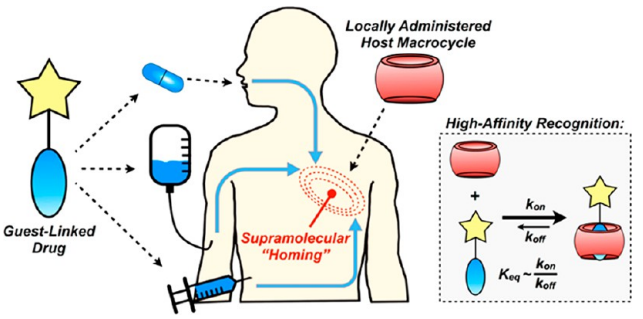

Figure 29. Schematic illustration of supramolecular homing of guest-appended small molecules based on the affinity for locally applied host macrocycles. Reprinted with permission from ref 114. Copyright 2019 American Chemical Society.

instantly form a hydrogel to precisely localize at a desired place, with the dangling CB[7] in the hydrogel acting as receptors for subsequently administered conjugates of guest molecules with fluorescent compounds or relevant drugs.

Considering whole cells, the modification of cell membranes has been realized thanks to functionalized β-cyclodextrins,[116] before being used for drug delivery.[117] With a macrocyclic ring and a hydrophobic cavity, functionalized CB[7] has also been used to modify cell membranes.[115] After addition of 1, 2-distearoyl-*sn*-glycero-3-phosphoethanolamine-PEG (DSPE-PEG) on CB[7] (**CB**[7]-**PEG-DSPE**, Figure 30), the conjugate was anchored on the cell membrane of macrophages, providing a multimodal platform for cell surface modification by simple addition of relevant compounds.

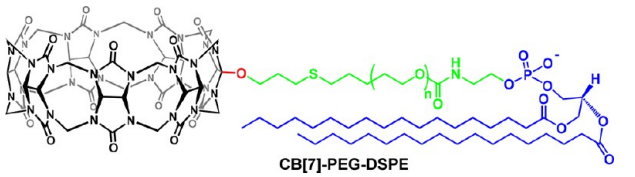

Figure 30. Chemical structure of **CB**[7]-**PEG-DSPE** (the functional group enables anchoring on the cell membrane).

Then, liposomes carrying various drugs were modified by DSPE-PEG-ADA to be attached to the surface of **CB**[7]-**macrophages**, owing to the strong host−guest interactions between the CB[7] and ADA units. The macrophages could lead drug-loaded liposomes up to inflamed tissues and release the drugs for augmented therapy. Following a similar strategy, **CB**[7]-**macrophages** were used to promote contact of *E. coli* preliminary coincubated with a mannose−ADA conjugate. The CB[7]•ADA recognition was again very powerful at bringing together the cells carrying the CB[7] and ADA fragments, thereby showing powerful antibacterial ability (Figure 31).[118]

Besides the modification of cell membranes, Wang and coworkers recently used **CB**[7]-**PEG-DSPE** and lecithin to construct **CB**[7]-**liposomes** for drug delivery.[119] Since polyamines are essential for tumor cell growth, they are often overexpressed and so considered as biomarkers in some types of cancers, such as breast and prostate cancers. Due to the strong binding affinity between CB[7] and polyamines, the CB[7]-functionalized liposomes showed high targeting efficiency toward 4T1 cells (a type of breast cancer cell line overexpressing polyamines). Tests in vivo on 4T1 cells-bearing mice demonstrated that CB[7]-functionalized liposomes

https://doi.org/10.1021/jacsau.3c00273
JACS Au 2023, 3, 2356−2377

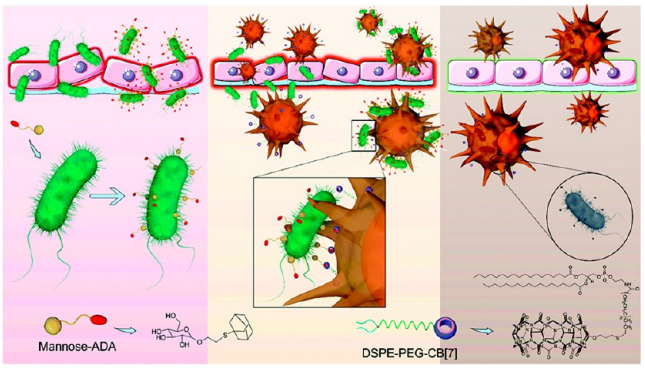

Figure 31. Supramolecular artificial receptor (SAR)−macrophages rapidly and specifically recognized *E. coli* through strong and multivalent host−guest interactions, thus improving the latching and internalization of *E. coli*, inducing M1 polarization of macrophages to generate ROS and effectively kill bacteria. Reprinted with permission from ref 118. Copyright 2022 Royal Society of Chemistry.

offered better tissue penetration and longer retention time in breast tumors. In the context of trauma and surgery, the control of coagulation is of tremendous importance and previous studies have shown the relevance of the supramolecular strategies.[120,121] Wang and co-workers developed CB[7]-functionalized platelets (SPLTs) based on hyaluronic acid-Von Willebrand factor-binding peptide (HA-VBP)-modified CB[7] (**CB[7]-HA-VBP**, Figure 32) and ADA-

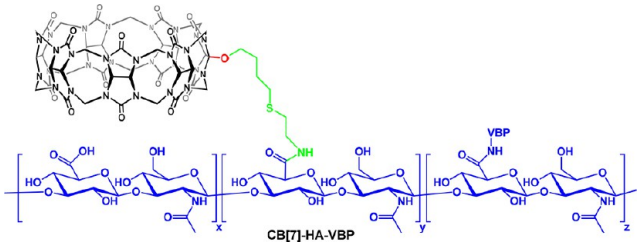

Figure 32. Chemical structure of **CB[7]-HA-VBP** (the functional group can promote the aggregation of PLTs to enhance hemostatic activity).

anchored platelets (ADA-PLTs).[122] This supramolecular combination showed an enhanced hemostatic activity with 1 order of magnitude better targeting efficiency compared to native PLTs, and less than 1/4 total bleeding time and 1/10 total bleeding volume compared to the control group.

Finally, Wang and co-workers used **CB[7]-HA** (Figure 33) loaded with curcumin to alleviate the symptoms of psoriasis,[123] relying both on the release of curcumin in cells and on

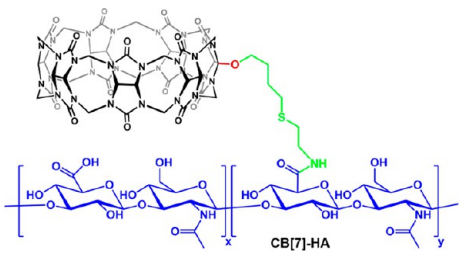

Figure 33. Chemical structure of **CB[7]-HA** (the functional group was introduced as scaffold for drug delivery).

polyamines sequestration, otherwise known to trigger inflammatory processes and exacerbate the disease.

5.4. F-CB[7]s for Biosensing

Unmodified CB[7] has regularly been used for biosensing, one of the main methods consisting of displacing a reporter dye from the cavity of the host.[11] This technique allowed for monitoring of enzymatic activity,[124] or translocation across lipid bilayer membranes.[125] To expand the scope of biological systems that can be studied by fluorescence using CB[7], several teams grafted different fluorophores on this host. For example, Nau, Hennig, and co-workers developed a host−guest FRET system based on carboxyfluorescein-modified CB[7] (**CB[7]-CF**, Figure 34) and DAPI for the sensing of DNA (Figure 35), reporting a new method to measure the concentration of DNA.[126] In 2022, challenges in detecting biorelevant metalobites incited Jochmann, Kappes, Biedermann, and co-workers to develop a nitrobenzofurazan-

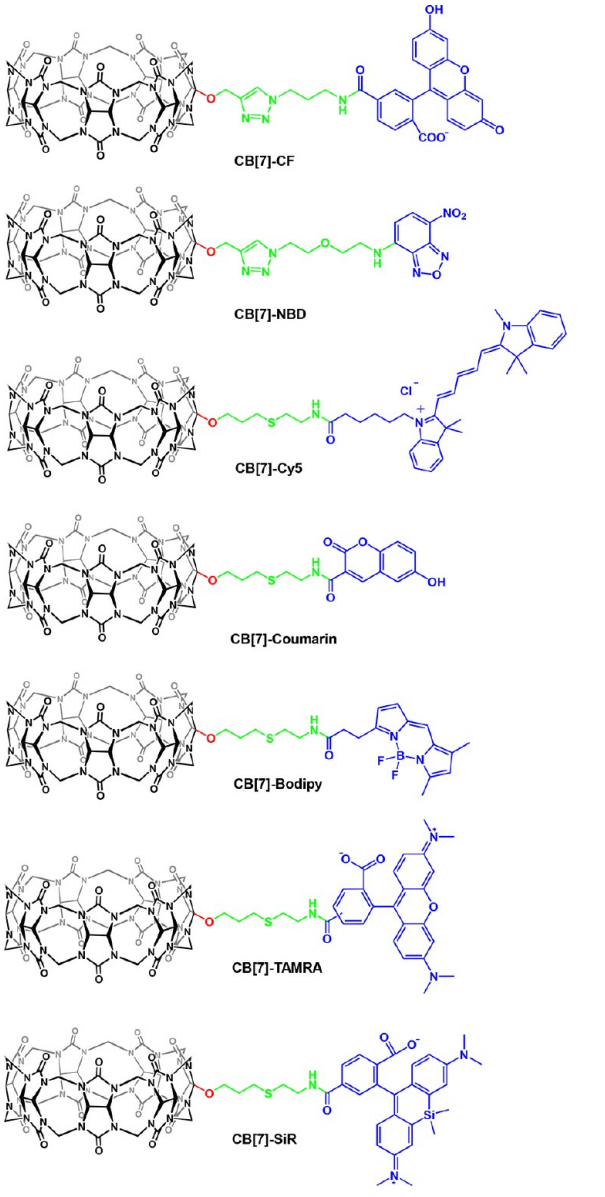

Figure 34. Chemical structures of **CB[7]-CF**, **CB[7]-NBD**, **CB[7]-Cy5**, **CB[7]-Coumarin**, **CB[7]-Bodipy**, **CB[7]-TAMRA**, and **CB[7]-SiR** (the functional groups were introduced as fluorescent indicators).

https://doi.org/10.1021/jacsau.3c00273
JACS Au 2023, 3, 2356−2377

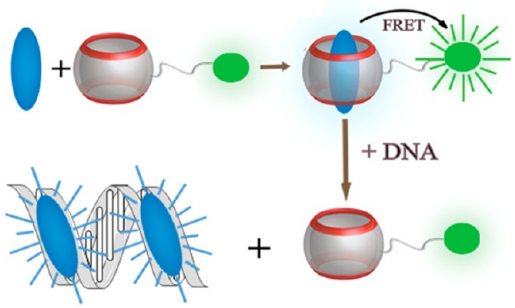

Figure 35. Schematic illustration of a DNA chemosensing ensemble based on FRET between DAPI (donor) and **CB7-CF** (acceptor). Reprinted with permission from ref 126. Copyright 2019 Royal Chemical Society.

functionalized CB[7] (**CB[7]-NBD**, Figure 34) used in array-based chemosensing methods to distinguishing 14 bioorganic analytes toward sensing in biofluids (Figure 36).[127]

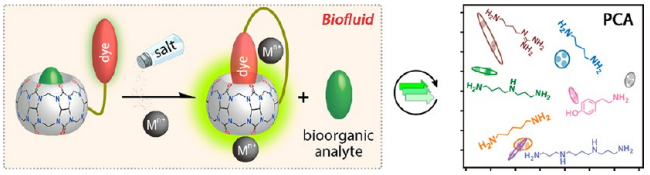

Figure 36. Schematic illustration of **CB[7]-NBD** as the key sensor used in array-based chemosensing to distinguish several bioorganic analytes in aqueous media and biofluids. Reprinted with permission from ref 127. Copyright 2022 American Chemical Society.

The same year, Gagey-Eilstein, Agasti, and co-workers synthesized a series of fluorophore-functionalized CB[7] (**CB[7]-Coumarin**, **CB[7]-Bodipy**, **CB[7]-Cy3**, **CB[7]-Cy5**, **CB[7]-TAMRA**, and **CB[7]-SiR**, Figure 34) as indicators to detect disease-specific amyloid assemblies,[128] which remains a daunting task.[129] This method not only enabled discrimination between different self-assembled forms of amyloid-β (Aβ) aggregates with high accuracy but was also applied successfully to predict clinically relevant changes (Figure 37).

5.5. *F*-CB[7]s for Controlled Release

Chen and co-workers reported in 2020 an original strategy for controlled drug release of a medicine encapsulated in **CB[7]-Hexanoate** (Figure 38).[130] The negatively charged carboxylate

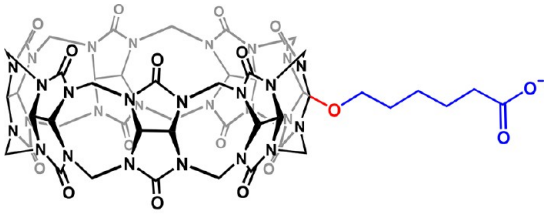

Figure 38. Chemical structure of **CB[7]-Hexanoate** (the functional group was introduced to enable pH responsive controlled release).

form is repelled from the CB[7] cavity, thereby preventing intermolecular association, the linker being presumably too short for self-inclusion. The cavity-free conjugate is thus amenable for drug binding. However, lowering pH by the

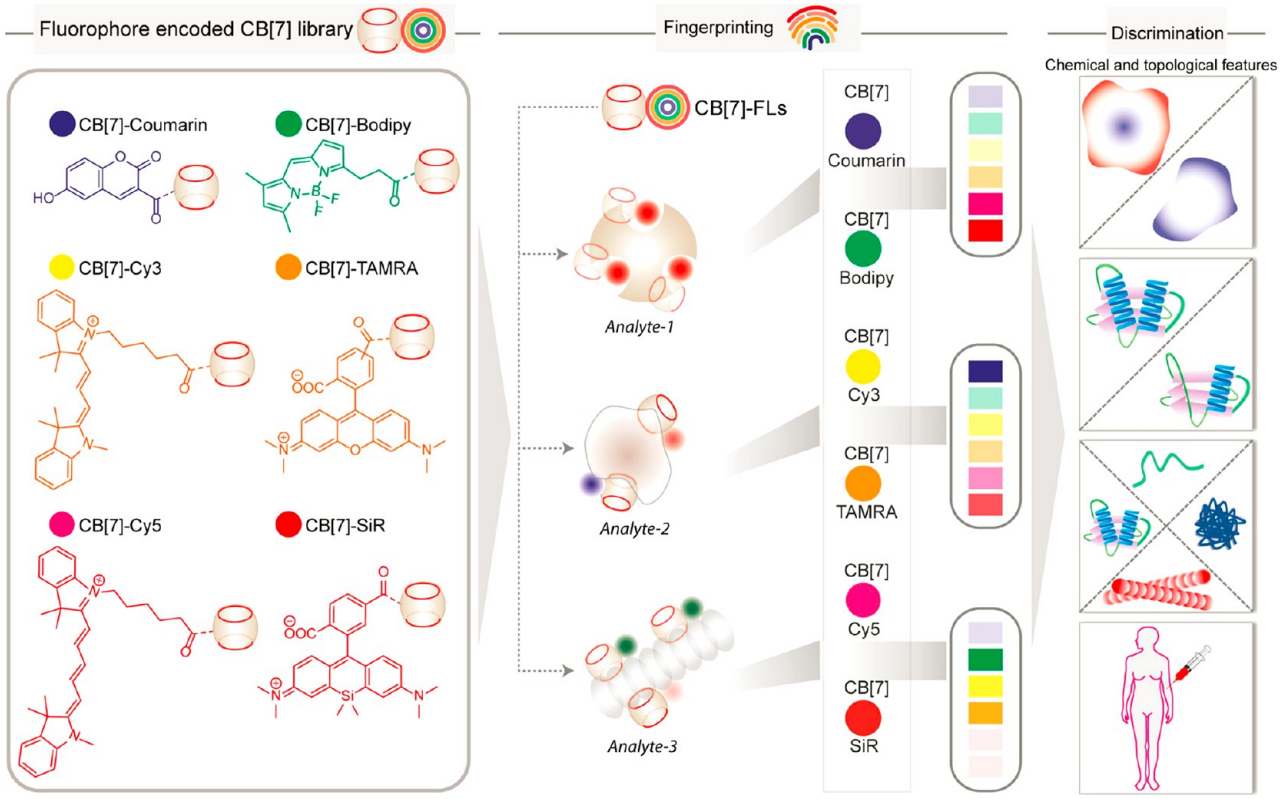

Figure 37. Strategy for fingerprinting biomolecular surfaces based on their chemical and topological features is based on fluorophore-linked CB[7] receptors. Reprinted with permission from ref 128. Copyright 2022 American Chemical Society.

https://doi.org/10.1021/jacsau.3c00273
JACS Au 2023, 3, 2356−2377

addition of acids protonates the carboxylate, affording a neutral form prone to self-inclusion in the CB[7] cavity by intermolecular associations and hence release of the previously encapsulated active compound. Despite the necessity for this *F*-CB[7] to match intermolecularly (which may be a drawback in vivo), this remarkably simple and effective way to encapsulate and release a bioactive compound should foster the tuning of the linker and the charge group as this should be a way to modulate the strength of aggregation or to propose intramolecular self-inclusion, and so expand the scope of bioactive compounds that could be transported and released.

6. APPLICATIONS OF *F*-CB[8]

Among the CB[*n*]s family, CB[8] has a relatively larger cavity size, which can accommodate large molecules or simultaneously bind two molecules, showing sizably different binding properties with respect to those possible with CB[6] or CB[7].[10] Compared to other macrocycles with large cavities, such as γ-cyclodextrin[131] or pillar[7]arene,[132] which have been functionalized, very few *F*-CB[8] have been reported, and only a couple of them were used for biological applications. Isaacs and co-workers managed to synthesize two CB[8] derivatives (**Me$_4$CB[8]** and **Cy$_2$CB[8]**, Figure 39) which were used to improve the solubility of several molecules,[57] benefiting from better solubilities of these derivatives compared to unmodified CB[8].

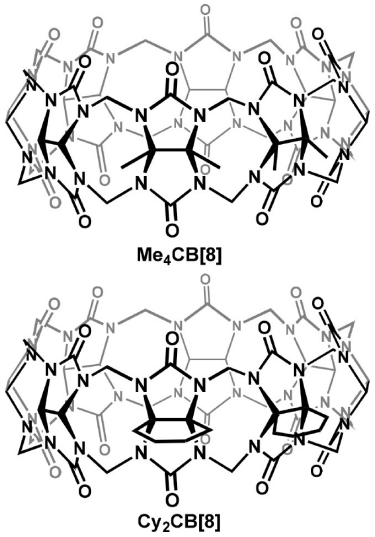

Figure 39. Chemical structures of **Me$_4$CB[8]** and **Cy$_2$CB[8]** (the functional groups were introduced to enhance solubility and modify binding properties).

This result could be explained by hampered self-association of the macrocycles in water[133] due to the presence of protruding alkyl groups. Recently, they demonstrated the Me$_4$CB[8] can act as an antidote toward a wide range of drugs of abuse,[58] the new host showing an especially strong binding affinity toward phencyclidine (PCP, $K_a = (5.35 \pm 0.19) \times 10^8$ M^{-1}). Subsequent in vivo studies suggested that Me$_4$CB[8] can be a potent antidote to prevent PCP-induced hyperlocomotion.

To enhance the solubility of CB[8], Ma and co-workers modified it, randomly substituting the peripheric C−H bonds by sulfonate groups.[134] Based on the substitution degree *n*, the following **CB[8]-Z$_n$** series (Figure 40) was obtained: **CB[8]-Z$_{3.18}$**, **CB[8]-Z$_{6.62}$**, and **CB[8]-Z$_{6.81}$**. Among these derivatives, **CB[8]-Z$_{3.81}$** proved to be the best binder (Table 1) toward a range of NMBAs, including cisatracurium besylate (CisA), rocuronium (Roc), vecuronium (Vec), pancuronium (Pan), and proflavine. With binding affinities reaching 10^7 M^{-1}, the neuromuscular block induced by CisA, Roc, Vec, and Pan can be efficiently reversed by encapsulation in **CB[8]-Z$_{3.18}$**, illustrating well its potential for clinical applications.

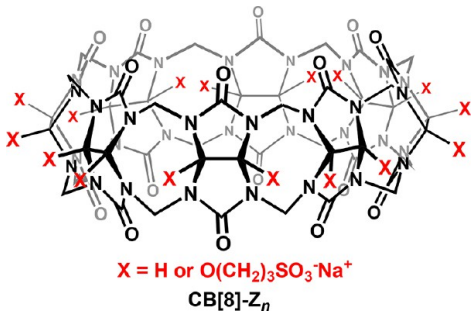

Figure 40. Chemical structure of **CB[8]-Z$_n$**, with *n* representing the calculated value for the number of functional groups (the functional groups were introduced to enhance solubility and modify binding properties).

7. CONCLUSION

While CB[5] has a small cavity amenable to bind only a small scope of compounds, CB[7] combined: (i) a relatively large cavity to bind a myriad of molecules, (ii) enough water solubility, and (iii) a relatively accessible functionalization. We can surmise that CB[6] and CB[8] are still difficult to functionalize owing to the relatively poor water solubility, and accordingly, a comparatively smaller number of studies involving *F*-CB[6] or *F*-CB[8]. Yet, considering these constraints, *F*-CB[*n*] is involved in a surprisingly high number of applications in biomedical sciences. Even if most studies must have taken time and effort, the combination of properties brought simultaneously by (i) the cavity of the macrocycle and (ii) the grafted function(s) has often enabled pushing forward frontiers impossible to overcome solely using a CB[*n*] and another molecule, noncovalently. While the main advances have been summarized in the previous section, fascinating perspectives remain to be explored like gene therapy, customized hydrogels, or molecularly imprinted polymers. Indeed, what makes the specificity of cucurbiturils is their high to ultrahigh guest binding in water, the solvent par excellence for biomedical applications of these well-tolerated compounds in vivo. Other macrocycles like calixarenes, cyclodextrins, or pillararenes, or more broadly supramolecular or covalent cages have allowed landmark achievements like specific DNA binding,[135] anion recognition,[136,137] or sugar recognition.[138] But these are endowed with neither the binding strength in water nor the versatility of bound systems, accessible by functionalized cucurbiturils.

8. KEY ADVANCES AND NEXT CHALLENGES

After initial findings of drug binding in the cavity of CB[7],[74,139] one could have questioned the added value of preparing functionalized CB[*n*]. Early intuitions have led to targeting cucurbiturils, the immediate benefit standing in the rational distribution of the host to specific cells or tissues and, by extension, of host−guest complexes once carrying suitable drugs. Even if particularly relevant to enable addressing a toxic

https://doi.org/10.1021/jacsau.3c00273
JACS Au 2023, 3, 2356−2377

Table 1. Summary Referencing the Functionalized CB[*n*], Their Access, Use, and Guest Molecules Used Bound in Their Cavity (CB[*n*] That Are Fluorescent Are Highlighted in Bold, Polymeric in Italic, and Binding Constants Determined for CB[7] are Underlined)

F-CB[*n*]	Synthesis	Application	Guest (K_a)[a]	Reference
CB[5]-$(OH)_{10}$	Direct	O_2 transport	O_2 (3.0×10^3 M^{-1})	60
CB[6]-polymer	Direct	Drug delivery	Galactose-spmd (N.D.)	66
CB[6]-polymer	Direct	Bioimaging	Spermidine (N.D.); FITC-spmd (N.D.); Cy7-spmd (N.D.); ^{64}Cu-NOTA-spmd (N.D.); cRGDyK-PEG-spmd (N.D.); PEG-spmd (N.D.)	67
CB[6]-polymer	Direct	Photodynamic therapy; Drug delivery	FA-SP (N.D.)	68
CB[6]-polymer	Direct	Drug delivery	FA-SP (N.D.)	69
CB[6]-polymer	Direct	Drug delivery	N.A.	70
CB[6]-*HA* CB[6]-Dexa	Direct	Tissue engineering	DAH-HA (N.D.)	72
CB[6]-AO	Direct	Biosensing	ACh^+ (N.D.)	73
CB[7]-biotin	X+1	Targeting	Oxaliplatin (5.0×10^8 M^{-1})	76
CB[7]-Ab	Direct	Targeting	ADA-Cy5 (N.D.)	77
CB[7]-M5A	N.A.	Targeting	[^{68}Ga]Ga-NOTA-PEG_3-NMe_2-Fc (N.D.)	78
CB[7]-VH4127	Direct	Targeting	ADA-A680	80
CB[7]-OH (bead)	Direct	Protein enrichment	AFc (N.D.)	82
CB[7]-OH (bead)	Direct	Protein enrichment	SAHA-Ad (N.D.)	83
CB[7]-OH (bead)	Direct	Protein enrichment	ADA-GGG (N.D.)	84
CB[7]-**Cy3**	Direct	Protein imaging; Bioimaging	FcA-COOH (N.D.); ADA-phenol (N.D.); ADA-BG (N.D.); ADA-COOH (N.D.)	51
CB[7]-**Cy3** CB[7]-Erbitux	Direct	Protein imaging; Bioimaging	ADA-BDP630/650 (N.D.) ADA-Cy5 (N.D.)	85
CB[7]-DNA	X+1	Binding mechanism	Ad-DNA (5.6×10^7 M^{-1} ~ 3.1×10^8 M^{-1})	88
CB[7]-DNA	X+1	Binding mechanism	Ad-Hexyl-DNA (N.D.); Ad^+-Hexyl-DNA (N.D.); Ad-Serinol-DNA (N.D.); Ad^+-Serinol-DNA (N.D.);	89
CB[7]-DNA	X+1	Binding mechanism	C6-Ad (~10^{10} M^{-1});	91
CB[7]-DNA	X+1	Biological regulation	Ad-benzenesulfonamide (~1.9×10^9 M^{-1}); Ad-DNA (~1.9×10^9 M^{-1})	90
CB[7]-**Cy3**	Direct	Bioimaging	Ad-Cy5 (N.D.)	86
CB[7]-**Cy3**	Direct	Bioimaging	Ad-Cy5 (N.D.)	87
CB[7]-*HA*	Direct	Biological regulation	TPP-PEG-ADA (N.D.)	52
CB[7]-**TMR**	X+1	Bioimaging	Phe-Gly-Gly (~2.8×10^6 M^{-1}); MV (6.25×10^6 M^{-1}); 1,6-Diaminohexane (~2.2×10^7 M^{-1}); 1,4-Bis(aminomethyl)benzene (~1.5×10^9 M^{-1})	93
CB[7]-*PEG*	X+1	Drug delivery	Insulin (~7×10^5 M^{-1})	94
CB[7]-*PEG*	X+1	Drug delivery	Insulin (1.85×10^6 M^{-1}); Pramlintide (2.63×10^4 M^{-1})	96
CB[7]-PEG polymer	Direct	Drug delivery	Oxaliplatin (1.8×10^6 M^{-1})	97
CB[7]-Bis(pyridine)	X+1	Drug delivery	HDA-$C_{18}H_{37}$ (8.97×10^7 M^{-1})	99
CB[7]-PLA	Direct	Drug delivery	PEG-ADA (N.D.); Oxaliplatin (N.D.); FA-ADA (N.D.); FITC-ADA (N.D.)	102
CB[7]-PLA	Direct	Drug delivery	PEG−PA-ADA (N.D.)	103
CB[7]-**AIE**	Direct	Bioimaging; Photodynamic therapy	Oxaliplatin (N.D.)	104
CB[7]-**AIE**	Direct	Bioimaging	AdLum (N.D.)	105
CB[7]-NH_2	Direct	Photothermal therapy; Drug delivery	FA-ADA (N.D.); Oxaliplatin (N.D.)	107
CB[7]-NH_2	Direct	Gene delivery; Drug delivery	PEG-ADA (N.D.); PLA-ADA (N.D.); HA-ADA (N.D.)	108
CB[7]-AO_1	Direct	Drug delivery	FA-ADA (N.D.); Oxaliplatin (N.D.)	109
CB[7]-AO_1	Direct	Bioimaging; Photothermal therapy	Au-Fc NPs (N.D.)	110

https://doi.org/10.1021/jacsau.3c00273
JACS Au 2023, 3, 2356−2377

Table 1. continued

F-CB[*n*]	Synthesis	Application	Guest (K_a)[a]	Reference
CB[7]-NH_2	Direct	Photothermal therapy; Photodynamic therapy; Drug delivery	Oxaliplatin (N.D.); HA-ADA (N.D.)	111
CB[7]-*PEG*-Ce6	Direct	Photodynamic therapy; Drug delivery	FA-ADA (N.D.)	113
CB[7]-*F127*-CB[7]	X+1	Drug delivery	PEG_8-Fc (3.5×10^{12} M^{-1}); Fc-O-Cy5 (9.5×10^{8} M^{-1}); Ad-Am-Cy5 (2.1×10^{10} M^{-1}); Fc-N-Cy5 (1.5×10^{12} M^{-1}); Fc-Hdz-Dox (N.A.)	114
CB[7]-PEG-DSPE	Direct	Drug delivery	DSPE-PEG-ADA (N.D.)	115
CB[7]-PEG-DSPE	Direct	Antibacterial	Mannose-ADA (N.D.)	118
CB[7]-PEG-DSPE	Direct	Drug delivery	SPMD (7.95×10^{5} M^{-1}); Spermine (2.02×10^{5} M^{-1}); Putrescine (1.45×10^{5} M^{-1})	119
CB[7]-*HA-VBP*	Direct	Biological regulation	DSPE-PEG-ADA (N.D.)	122
CB[7]-*HA*	Direct	Drug delivery	Curcumin (N.D.)	123
CB[7]-**CF**	Direct	Biosensing	DAPI (5.2×10^{6} M^{-1})	126
CB[7]-**NBD**	Direct	Biosensing	Putrescine (1.58×10^{5} M^{-1}); Cadaverine (1×10^{7} M^{-1}); SPMD (2.00×10^{6} M^{-1}); Spermine (6.31×10^{7} M^{-1}); Agmatine (3.16×10^{5} M^{-1}); Tyramine (6.31×10^{5} M^{-1}); ADA ($\geq 1 \times 10^{8}$ M^{-1}); Phe-Gly (1×10^{7} M^{-1}); Nandrolone (N.D.); MV (5.01×10^{6} M^{-1}); 1-adamantanol ($\geq 1 \times 10^{8}$ M^{-1}); Pinacol (1.58×10^{5} M^{-1}); 4F-PEA (2.51×10^{6} M^{-1}); C_8min ($\geq 1 \times 10^{8}$ M^{-1})	127
CB[7]-**Cy3** CB[7]-**Cy5** CB[7]-Coumarin CB[7]-**Bodipy** CB[7]-**TAMRA** CB[7]-**SiR**	Direct	Biosensing	Proteins (N.D.)	128
CB[8]-$(Me)_4$ CB[8]-$(Cy)_2$	X+1	Solubility increase	CB[8]-$(Me)_4$: Amiodarone (1.21×10^{4} M^{-1}); Tamoxifen (4.67×10^{4} M^{-1}); β-Estradiol (1.07×10^{4} M^{-1}); Albendazole (2.21×10^{5} M^{-1})	57
CB[8]-$(Me)_4$	X+1	Toxicity decrease	Meth (2.98×10^{4} M^{-1}); Fentanyl (1.98×10^{6} M^{-1} for 1:1 binding and (9.52×10^{4} M^{-1} for 2:1 binding); Morphine (4.67×10^{7} M^{-1}); Hydromorphone (2.14×10^{7} M^{-1}); Ketamine (2.81×10^{7} M^{-1}); PCP (5.35×10^{8} M^{-1}); Cocaine (2.77×10^{5} M^{-1}); Cycloheptylamine (1.04×10^{6} M^{-1}); Cyclooctylamine (2.79×10^{6} M^{-1}); MDMA (3.13×10^{4} M^{-1}); Mephedrone (3.07×10^{5} M^{-1}); Heroin (7.94×10^{4} M^{-1})	58
CB[8]-$Z_{3.18}$	Direct	Neuromuscular blocking reversal	CisA (1.08×10^{7} M^{-1}); Roc (1.97×10^{7} M^{-1}); Vec (2.15×10^{7} M^{-1}); Pan (1.72×10^{7} M^{-1}); proflavine (1.4×10^{6} M^{-1})	134
CB[8]-$Z_{6.62}$			CisA (6.5×10^{5} M-1); Roc (1.1×10^{6} M^{-1}); Vec (9.2×10^{5} M^{-1}); Pan (1.0×10^{6} M^{-1}); proflavine (6.9×10^{4} M^{-1})	
CB[8]-$Z_{6.81}$			CisA (3.3×10^{5} M^{-1}); proflavine (3.8×10^{4} M^{-1})	

[a]N.A.: Not available. N.D.: Not determined.

https://doi.org/10.1021/jacsau.3c00273
JACS Au 2023, 3, 2356−2377

or bioactive compound to a specific location (i.e., tumors, inflamed tissues, or organ-specific diseases), therefore preserving healthy cells, this approach remains largely unexplored. Even so, after about two decades and starting from laboratory curiosities, the field of functionalized cucurbiturils has grown to a mature research area, key findings having enabled unclocking of troublesome bottlenecks (essentially functionalization methods). The protocols now available, even if still far from perfect (yields for monofunctional compounds and purification methods can, and should, be improved), have enabled preparation of a myriad of CB derivatives having shown a plethora of interesting properties. More specifically:

- CB[5]-$(OH)_{10}$ has shown a great potential for oxygen transport which could open the way to a potent artificial hemoglobin.[60] It would now be interesting to check its toxicity in detail and investigate this behavior in vivo. The scope of guests fitting in the cavity is here reduced, but there are still several interesting molecules to be trapped in the cavity of a CB[5] that may benefit from macrocycle surface functionalization (i.e., targeting).
- Functionalized CB[6] has mainly be used to prepare nanocapsules used in various applications of biomedical relevance (principally compound capture and release, and in theranostics).[66−70] Yet, there are much fewer derivatives than for *F*-CB[7]; a reason could be the remaining rather low solubility of *F*-CB[6] hampering further use in water. However, managing to prepare water-soluble and functional *F*-CB[6] could open the way to many unique applications of CB[6] due to the specific size and shape of its cavity. It is also the more easily obtained cucurbituril, in high amounts, and much easier to functionalize by a hydroxyl group.
- Functionalized CB[7] have first been used for cell targeting in a biomedical context,[76−79] but strangely, few works have been done in this direction since. Yet targeting can add a great value to CB[7], toward specific tissue distribution in vivo, thereby enhancing therapeutic efficacy and decreasing side-effects of complexed drugs. But perhaps the most important advance in this field is the reliable use of the CB[7]•ADA or CB[7]•Fc pair to attract or glue together two tethered entities. As anticipated quite early by some researchers,[140,141] the ultrahigh affinity of CB[7] for ADA or Fc amino derivatives enabled to strongly (though dynamically) link together (i) polymer beads and proteins, (ii) DNA strands, (iii) mitochondria, or even (iv) cells, to cite but a few examples. The CB[7]-bead system has enabled several advances and by this has established its potential.[82−84] Again, there remains to do a lot in this direction (i.e., specific cell isolation, purification, or in nanomedicine). Fluorescent CB[7] (by grafting of fluorophores) have been widely used (i.e., for protein location in living cells,[51] monitoring of membrane fusion,[86,87] following CB[7] cell uptake,[93] deep-tissue-inflammation imaging,[105] quantitative DNA sensing,[126] bioorganic analyte sensing,[127] or predicting protein structural changes).[128] The CB[7]•ADA pair is so stable that it can easily sustain the conditions encountered in cells. It has thus been instrumental to dramatically expand the possibilities offered by CB[7] in vivo. We can anticipate that many more fluorescent CB[7] will be prepared and used in the future, and many more systems using the CB[7]•ADA pair will be used in chemistry and biology. DNA-CB[7] conjugates have enabled the determination of the strength of supramolecular interactions by a new method,[88,89] and an ATP-fueled method was developed for selective protein inhibitor release after DNA duplex formation.[90] Considering the huge developments in the domain of DNA (i.e., DNA origami,[142] wireframe assembly,[143] tile assembly[144]), we can bet for unique combinations and properties once the DNA assembly will have been combined with the specific features of the ultrahigh-affinity bonds provided by the CB[7]•ADA pair. The supramolecular PEGylation of proteins by CB[7]-PEG conjugates has also been shown to improve the pharmacokinetics of insulin and pramlintide,[96] while CB[7]-NH_2 was used in nanomedicine[107,108,111] and CB[7]-allyl assemblies in drug release.[109] The field of nanomedicine has particularly benefited from *F*-CB[7] (chemotherapy,[113] photothermal therapy,[107,110,111] photodynamic therapy,[104,111,113] gene therapy,[108] as well as synergistic combinations of these). Of note, functionalized CB[7] has rarely been interfaced with metal−ligand complexes, a notable example being the CB[7]-decorated MOP cages benefiting from the surface binding provided by the grafted macrocycles.[99] If we consider the great developments over the last decades of metallo-supramolecular chemistry,[145,146] we can easily imagine a wealth of opportunities to explore at this interface (i.e., with helicates,[147] grids,[148] foldamers,[149] metallogels,[150] or catenated structures[151,152]). Likewise, CB[7] containing polymers have little been applied to the biomedical field (chemotherapy,[97] supramolecularly functionalized platelets).[122] Many more applications of such conjugates are expected in the future (i.e., cyclic polymers, antibacterial, gene delivery). Finally, the opportunity to tune cell surfaces thanks to anchored CB[7] on relevant membranes[115,118] has also opened the door to cellular biology. With few exceptions, all these works could not have been done without CB[7] functionalization. Finally, molecular motors are topical systems,[153] and very little has been done toward cucurbituril molecular motors.[154−156] Yet natural molecular motors are ubiquitous in biology, bringing pivotal functions for cell machinery.[157] We can anticipate that, when the assembly of cucurbituril-based molecular motors will have been mastered, new avenues will be opened toward influencing natural molecular machines, or creating new functions. There are few doubts that when this will happen, *F*-CB[7] will play crucial roles.
- Compared to *F*-CB[7], functionalized CB[8] are still quite exotic compounds, CB[8] being very hard to functionalize, and also relatively weakly soluble. CB[8]-$(Me)_4$ and CB[8]-$(Cy)_2$ have been investigated as soluble hosts to improve the solubility of hydrophobic drugs. The small number of derivatives used in biological applications illustrates quite well the daunting task of functionalizing CB[8]. Yet, if we consider the developments CB[8] brought already by itself in the biomedical field (i.e., supramolecular protein dimerization,[158] enzymatic activity sensing,[159] drug delivery,[160] and biomaterials construction)[161] and the specificity of its cavity for two planar aromatic guest fragments or globular fragments, larger than those usually bound by

https://doi.org/10.1021/jacsau.3c00273
JACS Au 2023, 3, 2356−2377

CB[7], there are no doubts about the number of possibilities remaining to be explored if the CB[8] functionalization can be unlocked (i.e., targeting, additional functions provided to host-stabilized hetero-guest pairs, or labeled-CB[8] for host-mediated protein dimerization, oligomerization of polymerization, mimicking the widely seen ring-shape protein aggregates).

AUTHOR INFORMATION

Corresponding Authors

Ruibing Wang − *State Key Laboratory of Quality Research in Chinese Medicine, Institute of Chinese Medical Sciences, University of Macau, Taipa, Macau 999078, China;* orcid.org/0000-0001-9489-4241; Email: rwang@um.edu.mo

David Bardelang − *CNRS, ICR, Aix Marseille Univ, 13013 Marseille, France;* orcid.org/0000-0002-0318-5958; Email: david.bardelang@univ-amu.fr

Authors

Hang Yin − *State Key Laboratory of Quality Research in Chinese Medicine, Institute of Chinese Medical Sciences, University of Macau, Taipa, Macau 999078, China;* orcid.org/0000-0002-2898-844X

Qian Cheng − *State Key Laboratory of Quality Research in Chinese Medicine, Institute of Chinese Medical Sciences, University of Macau, Taipa, Macau 999078, China*

Complete contact information is available at: https://pubs.acs.org/10.1021/jacsau.3c00273

Author Contributions

#These authors contributed equally. The manuscript was written through contributions of all authors.

Notes

The authors declare no competing financial interest.

ACKNOWLEDGMENTS

We greatly acknowledge the following funding bodies: University of Macau Multi-Year Research Grant (MYRG-CRG2022-00011-ICMS and MYRG2022-00081-ICMS), the Science and Technology Development Fund (FDCT) of Macau SAR (SKL-QRCM(UM)-2023-2025, 0086/2022/A2, and 0065/2021/A2), Shenzhen Science and Technology Innovation Commission (EF023/ICMS-WRB/2022/SZSTIC), and the National Natural Science Foundation of China (22071275 and 22271323), as well as the University of Macau − Dr. Stanley Ho Medical Development Foundation "Set Sail for New Horizons, Create the Future" Grant (SHMDF-VSEP/2022/001). Aix-Marseille University and CNRS are acknowledged for continuous support.

REFERENCES

(1) Murray, J.; Kim, K.; Ogoshi, T.; Yao, W.; Gibb, B. C. The aqueous supramolecular chemistry of cucurbit[n]urils, pillar[n]arenes and deep-cavity cavitands. *Chem. Soc. Rev.* **2017**, *46*, 2479−2496.

(2) Steed, J. W.; Atwood, J. L. *Supramolecular chemistry*. John Wiley & Sons, 2022.

(3) Vögtle, F.; Weber, E. *Host Guest Complex Chemistry Macrocycles: Synthesis, Structures, Applications*. Springer Science & Business Media, 2012.

(4) Dong, S.; Zheng, B.; Wang, F.; Huang, F. Supramolecular Polymers Constructed from Macrocycle-Based Host−Guest Molecular Recognition Motifs. *Acc. Chem. Res.* **2014**, *47*, 1982−1994.

(5) Dsouza, R. N.; Pischel, U.; Nau, W. M. Fluorescent Dyes and Their Supramolecular Host/Guest Complexes with Macrocycles in Aqueous Solution. *Chem. Rev.* **2011**, *111*, 7941−7980.

(6) Kim, J.; Jung, I.-S.; Kim, S.-Y.; Lee, E.; Kang, J.-K.; Sakamoto, S.; Yamaguchi, K.; Kim, K. New Cucurbituril Homologues: Syntheses, Isolation, Characterization, and X-ray Crystal Structures of Cucurbit[n]uril (n = 5, 7, and 8). *J. Am. Chem. Soc.* **2000**, *122*, 540−541.

(7) Day, A.; Arnold, A.; Blanch, R. Method for synthesis cucurbiturils. WO2000068232A1, 2000.

(8) Lee, J. W.; Samal, S.; Selvapalam, N.; Kim, H.-J.; Kim, K. Cucurbituril Homologues and Derivatives: New Opportunities in Supramolecular Chemistry. *Acc. Chem. Res.* **2003**, *36*, 621−630.

(9) Lagona, J.; Mukhopadhyay, P.; Chakrabarti, S.; Isaacs, L. The Cucurbit[n]uril Family. *Angew. Chem., Int. Ed.* **2005**, *44*, 4844−4870.

(10) Barrow, S. J.; Kasera, S.; Rowland, M. J.; del Barrio, J.; Scherman, O. A. Cucurbituril-Based Molecular Recognition. *Chem. Rev.* **2015**, *115*, 12320−12406.

(11) Assaf, K. I.; Nau, W. M. Cucurbiturils: from synthesis to high-affinity binding and catalysis. *Chem. Soc. Rev.* **2015**, *44*, 394−418.

(12) Masson, E.; Ling, X.; Joseph, R.; Kyeremeh-Mensah, L.; Lu, X. Cucurbituril chemistry: a tale of supramolecular success. *RSC Adv.* **2012**, *2*, 1213−1247.

(13) Urbach, A. R.; Ramalingam, V. Molecular Recognition of Amino Acids, Peptides, and Proteins by Cucurbit[n]uril Receptors. *Isr. J. Chem.* **2011**, *51*, 664−678.

(14) Yin, H.; Wang, R. Applications of Cucurbit[n]urils (n = 7 or 8) in Pharmaceutical Sciences and Complexation of Biomolecules. *Isr. J. Chem.* **2018**, *58*, 188−198.

(15) Yin, H.; Bardelang, D.; Wang, R. Macrocycles and Related Hosts as Supramolecular Antidotes. *Trends in Chemistry* **2021**, *3*, 1−4.

(16) Deng, C.-L.; Murkli, S. L.; Isaacs, L. D. Supramolecular hosts as in vivo sequestration agents for pharmaceuticals and toxins. *Chem. Soc. Rev.* **2020**, *49*, 7516−7532.

(17) Yin, H.; Zhang, X.; Wei, J.; Lu, S.; Bardelang, D.; Wang, R. Recent advances in supramolecular antidotes. *Theranostics* **2021**, *11*, 1513−1526.

(18) Zhao, Y.; Buck, D. P.; Morris, D. L.; Pourgholami, M. H.; Day, A. I.; Collins, J. G. Solubilisation and cytotoxicity of albendazole encapsulated in cucurbit[n]uril. *Organic & Biomolecular Chemistry* **2008**, *6*, 4509−4515.

(19) Li, S.; Chan, J. Y.-W.; Li, Y.; Bardelang, D.; Zheng, J.; Yew, W. W.; Chan, D. P.-C.; Lee, S. M. Y.; Wang, R. Complexation of clofazimine by macrocyclic cucurbit[7]uril reduced its cardiotoxicity without affecting the antimycobacterial efficacy. *Organic & Biomolecular Chemistry* **2016**, *14*, 7563−7569.

(20) Yang, X.; Huang, Q.; Bardelang, D.; Wang, C.; Lee, S. M. Y.; Wang, R. Supramolecular alleviation of cardiotoxicity of a small-molecule kinase inhibitor. *Organic & Biomolecular Chemistry* **2017**, *15*, 8046−8053.

(21) Li, W.; Yin, H.; Bardelang, D.; Xiao, J.; Zheng, Y.; Wang, R. Supramolecular formulation of nitidine chloride can alleviate its hepatotoxicity and improve its anticancer activity. *Food Chem. Toxicol.* **2017**, *109*, 923−929.

(22) Zhang, X.; Xu, X.; Li, S.; Li, L.; Zhang, J.; Wang, R. A Synthetic Receptor as a Specific Antidote for Paraquat Poisoning. *Theranostics* **2019**, *9*, 633−645.

(23) Zhang, X.; Huang, Q.; Zhao, Z.-Z.; Xu, X.; Li, S.; Yin, H.; Li, L.; Zhang, J.; Wang, R. An Eco- and User-Friendly Herbicide. *J. Agric. Food Chem.* **2019**, *67*, 7783−7792.

(24) Bellia, F.; La Mendola, D.; Pedone, C.; Rizzarelli, E.; Saviano, M.; Vecchio, G. Selectively functionalized cyclodextrins and their metal complexes. *Chem. Soc. Rev.* **2009**, *38*, 2756−2781.

(25) Zhou, J.; Ritter, H. Cyclodextrin functionalized polymers as drug delivery systems. *Polym. Chem.* **2010**, *1*, 1552−1559.

(26) Nimse, S. B.; Kim, T. Biological applications of functionalized calixarenes. *Chem. Soc. Rev.* **2013**, *42*, 366−386.

(27) Yu, G.; Xue, M.; Zhang, Z.; Li, J.; Han, C.; Huang, F. A Water-Soluble Pillar[6]arene: Synthesis, Host−Guest Chemistry, and Its Application in Dispersion of Multiwalled Carbon Nanotubes in Water. *J. Am. Chem. Soc.* **2012**, *134*, 13248−13251.
(28) Xue, W.; Zavalij, P. Y.; Isaacs, L. Pillar[n]MaxQ: A New High Affinity Host Family for Sequestration in Water. *Angew. Chem., Int. Ed.* **2020**, *59*, 13313−13319.
(29) Shih, H.; Lin, C.-C. Photoclick Hydrogels Prepared from Functionalized Cyclodextrin and Poly(ethylene glycol) for Drug Delivery and in Situ Cell Encapsulation. *Biomacromolecules* **2015**, *16*, 1915−1923.
(30) Zhang, X.; Cheng, Q.; Li, L.; Shangguan, L.; Li, C.; Li, S.; Huang, F.; Zhang, J.; Wang, R. Supramolecular therapeutics to treat the side effects induced by a depolarizing neuromuscular blocking agent. *Theranostics* **2019**, *9*, 3107−3121.
(31) Bom, A.; Bradley, M.; Cameron, K.; Clark, J. K.; van Egmond, J.; Feilden, H.; MacLean, E. J.; Muir, A. W.; Palin, R.; Rees, D. C.; Zhang, M.-Q. A Novel Concept of Reversing Neuromuscular Block: Chemical Encapsulation of Rocuronium Bromide by a Cyclodextrin-Based Synthetic Host. *Angew. Chem., Int. Ed.* **2002**, *41*, 265−270.
(32) Adam, J. M.; Bennett, D. J.; Bom, A.; Clark, J. K.; Feilden, H.; Hutchinson, E. J.; Palin, R.; Prosser, A.; Rees, D. C.; Rosair, G. M.; Stevenson, D.; Tarver, G. J.; Zhang, M.-Q. Cyclodextrin-Derived Host Molecules as Reversal Agents for the Neuromuscular Blocker Rocuronium Bromide: Synthesis and Structure-Activity Relationships. *J. Med. Chem.* **2002**, *45*, 1806−1816.
(33) Guo, D.-S.; Liu, Y. Supramolecular Chemistry of p-Sulfonatocalix[n]arenes and Its Biological Applications. *Acc. Chem. Res.* **2014**, *47*, 1925−1934.
(34) Yu, G.; Zhou, X.; Zhang, Z.; Han, C.; Mao, Z.; Gao, C.; Huang, F. Pillar[6]arene/Paraquat Molecular Recognition in Water: High Binding Strength, pH-Responsiveness, and Application in Controllable Self-Assembly, Controlled Release, and Treatment of Paraquat Poisoning. *J. Am. Chem. Soc.* **2012**, *134*, 19489−19497.
(35) Huang, W.-H.; Zavalij, P. Y.; Isaacs, L. Cucurbit[n]uril Formation Proceeds by Step-Growth Cyclo-oligomerization. *J. Am. Chem. Soc.* **2008**, *130*, 8446−8454.
(36) Cong, H.; Ni, X. L.; Xiao, X.; Huang, Y.; Zhu, Q.-J.; Xue, S.-F.; Tao, Z.; Lindoy, L. F.; Wei, G. Synthesis and separation of cucurbit[n]urils and their derivatives. *Organic & Biomolecular Chemistry* **2016**, *14*, 4335−4364.
(37) Zhao, W.-X.; Wang, C.-Z.; Chen, L.-X.; Cong, H.; Xiao, X.; Zhang, Y.-Q.; Xue, S.-F.; Huang, Y.; Tao, Z.; Zhu, Q.-J. A Hemimethyl-Substituted Cucurbit[7]uril Derived from 3α-Methylglycoluril. *Org. Lett.* **2015**, *17*, 5072−5075.
(38) Yang, X.; Zhao, W.; Wang, Z.; Huang, Y.; Lee, S. M. Y.; Tao, Z.; Wang, R. Toxicity of hemimethyl-substituted cucurbit[7]uril. *Food Chem. Toxicol.* **2017**, *108*, 510−518.
(39) Zhao, Y.; Mandadapu, V.; Iranmanesh, H.; Beves, J. E.; Day, A. I. The Inheritance Angle: A Determinant for the Number of Members in the Substituted Cucurbit[n]uril Family. *Org. Lett.* **2017**, *19*, 4034−4037.
(40) Wu, A.; Chakraborty, A.; Witt, D.; Lagona, J.; Damkaci, F.; Ofori, M. A.; Chiles, J. K.; Fettinger, J. C.; Isaacs, L. Methylene-Bridged Glycoluril Dimers: Synthetic Methods. *Journal of Organic Chemistry* **2002**, *67*, 5817−5830.
(41) Jon, S. Y.; Selvapalam, N.; Oh, D. H.; Kang, J.-K.; Kim, S.-Y.; Jeon, Y. J.; Lee, J. W.; Kim, K. Facile Synthesis of Cucurbit[n]uril Derivatives via Direct Functionalization: Expanding Utilization of Cucurbit[n]uril. *J. Am. Chem. Soc.* **2003**, *125*, 10186−10187.
(42) Ayhan, M. M.; Karoui, H.; Hardy, M.; Rockenbauer, A.; Charles, L.; Rosas, R.; Udachin, K.; Tordo, P.; Bardelang, D.; Ouari, O. Comprehensive Synthesis of Monohydroxy−Cucurbit[n]urils (n = 5, 6, 7, 8): High Purity and High Conversions. *J. Am. Chem. Soc.* **2015**, *137*, 10238−10245.
(43) Gilberg, L.; Khan, M. S. A.; Enderesova, M.; Sindelar, V. Cucurbiturils Substituted on the Methylene Bridge. *Org. Lett.* **2014**, *16*, 2446−2449.
(44) Zhao, N.; Lloyd, G. O.; Scherman, O. A. Monofunctionalised cucurbit[6]uril synthesis using imidazolium host−guest complexation. *Chem. Commun.* **2012**, *48*, 3070−3072.
(45) Ahn, Y.; Jang, Y.; Selvapalam, N.; Yun, G.; Kim, K. Supramolecular Velcro for Reversible Underwater Adhesion. *Angew. Chem., Int. Ed.* **2013**, *52*, 3140−3144.
(46) Park, K. M.; Baek, K.; Ko, Y. H.; Shrinidhi, A.; Murray, J.; Jang, W. H.; Kim, K. H.; Lee, J.-S.; Yoo, J.; Kim, S.; Kim, K. Mono-allyloxylated Cucurbit[7]uril Acts as an Unconventional Amphiphile To Form Light-Responsive Vesicles. *Angew. Chem., Int. Ed.* **2018**, *57*, 3132−3136.
(47) Ghosh, S. K.; Dhamija, A.; Ko, Y. H.; An, J.; Hur, M. Y.; Boraste, D. R.; Seo, J.; Lee, E.; Park, K. M.; Kim, K. Superacid-Mediated Functionalization of Hydroxylated Cucurbit[n]urils. *J. Am. Chem. Soc.* **2019**, *141*, 17503−17506.
(48) Ayhan, M. M.; Karoui, H.; Hardy, M.; Rockenbauer, A.; Charles, L.; Rosas, R.; Udachin, K.; Tordo, P.; Bardelang, D.; Ouari, O. Correction to "Comprehensive Synthesis of Monohydroxy−Cucurbit[n]urils (n = 5, 6, 7, 8): High Purity and High Conversions. *J. Am. Chem. Soc.* **2016**, *138*, 2060−2060.
(49) Shen, F.-F.; Chen, K.; Zhang, Y.-Q.; Zhu, Q.-J.; Tao, Z.; Cong, H. Mono- and Dihydroxylated Symmetrical Octamethylcucurbiturils and Allylated Derivatives. *Org. Lett.* **2016**, *18*, 5544−5547.
(50) Gao, R. H.; Chen, L. X.; Chen, K.; Tao, Z.; Xiao, X. Development of hydroxylated cucurbit[n]urils, their derivatives and potential applications. *Coord. Chem. Rev.* **2017**, *348*, 1−24.
(51) Kim, K. L.; Sung, G.; Sim, J.; Murray, J.; Li, M.; Lee, A.; Shrinidhi, A.; Park, K. M.; Kim, K. Supramolecular latching system based on ultrastable synthetic binding pairs as versatile tools for protein imaging. *Nat. Commun.* **2018**, *9*, 1712.
(52) Sun, C.; Wang, Z.; Yue, L.; Huang, Q.; Cheng, Q.; Wang, R. Supramolecular Induction of Mitochondrial Aggregation and Fusion. *J. Am. Chem. Soc.* **2020**, *142*, 16523−16527.
(53) Kataki-Anastasakou, A.; Axtell, J. C.; Hernandez, S.; Dziedzic, R. M.; Balaich, G. J.; Rheingold, A. L.; Spokoyny, A. M.; Sletten, E. M. Carborane Guests for Cucurbit[7]uril Facilitate Strong Binding and On-Demand Removal. *J. Am. Chem. Soc.* **2020**, *142*, 20513−20518.
(54) Cao, L.; Isaacs, L. Daisy Chain Assembly Formed from a Cucurbit[6]uril Derivative. *Org. Lett.* **2012**, *14*, 3072−3075.
(55) Vinciguerra, B.; Cao, L.; Cannon, J. R.; Zavalij, P. Y.; Fenselau, C.; Isaacs, L. Synthesis and Self-Assembly Processes of Monofunctionalized Cucurbit[7]uril. *J. Am. Chem. Soc.* **2012**, *134*, 13133−13140.
(56) Ma, D.; Hettiarachchi, G.; Nguyen, D.; Zhang, B.; Wittenberg, J. B.; Zavalij, P. Y.; Briken, V.; Isaacs, L. Acyclic cucurbit[n]uril molecular containers enhance the solubility and bioactivity of poorly soluble pharmaceuticals. *Nat. Chem.* **2012**, *4*, 503−510.
(57) Vinciguerra, B.; Zavalij, P. Y.; Isaacs, L. Synthesis and Recognition Properties of Cucurbit[8]uril Derivatives. *Org. Lett.* **2015**, *17*, 5068−5071.
(58) Murkli, S.; Klemm, J.; Brockett, A. T.; Shuster, M.; Briken, V.; Roesch, M. R.; Isaacs, L. In Vitro and In Vivo Sequestration of Phencyclidine by Me4Cucurbit[8]uril**. *Chemistry − A European Journal* **2021**, *27*, 3098−3105.
(59) Miyahara, Y.; Abe, K.; Inazu, T. Molecular" Molecular Sieves: Lid-Free Decamethylcucurbit[5]uril Absorbs and Desorbs Gases Selectively. *Angew. Chem., Int. Ed.* **2002**, *41*, 3020−3023.
(60) Huber, G.; Berthault, P.; Nguyen, A. L.; Pruvost, A.; Barruet, E.; Rivollier, J.; Heck, M.-P.; Prieur, B. Cucurbit[5]uril derivatives as oxygen carriers. *Supramol. Chem.* **2019**, *31*, 668−675.
(61) Mock, W. L.; Shih, N. Y. Structure and selectivity in host-guest complexes of cucurbituril. *Journal of Organic Chemistry* **1986**, *51*, 4440−4446.
(62) Lee, H.-K.; Park, K. M.; Jeon, Y. J.; Kim, D.; Oh, D. H.; Kim, H. S.; Park, C. K.; Kim, K. Vesicle Formed by Amphiphilc Cucurbit[6]-uril: Versatile, Noncovalent Modification of the Vesicle Surface, and Multivalent Binding of Sugar-Decorated Vesicles to Lectin. *J. Am. Chem. Soc.* **2005**, *127*, 5006−5007.

https://doi.org/10.1021/jacsau.3c00273
JACS Au 2023, 3, 2356−2377

(63) Kim, D.; Kim, E.; Kim, J.; Park, K. M.; Baek, K.; Jung, M.; Ko, Y. H.; Sung, W.; Kim, H. S.; Suh, J. H.; Park, C. G.; Na, O. S.; Lee, D.-k.; Lee, K. E.; Han, S. S.; Kim, K. Direct Synthesis of Polymer Nanocapsules with a Noncovalently Tailorable Surface. *Angew. Chem., Int. Ed.* **2007**, *46*, 3471−3474.
(64) Kim, D.; Kim, E.; Lee, J.; Hong, S.; Sung, W.; Lim, N.; Park, C. G.; Kim, K. Direct Synthesis of Polymer Nanocapsules: Self-Assembly of Polymer Hollow Spheres through Irreversible Covalent Bond Formation. *J. Am. Chem. Soc.* **2010**, *132*, 9908−9919.
(65) Baek, K.; Yun, G.; Kim, Y.; Kim, D.; Hota, R.; Hwang, I.; Xu, D.; Ko, Y. H.; Gu, G. H.; Suh, J. H.; Park, C. G.; Sung, B. J.; Kim, K. Free-Standing, Single-Monomer-Thick Two-Dimensional Polymers through Covalent Self-Assembly in Solution. *J. Am. Chem. Soc.* **2013**, *135*, 6523−6528.
(66) Kim, E.; Kim, D.; Jung, H.; Lee, J.; Paul, S.; Selvapalam, N.; Yang, Y.; Lim, N.; Park, C. G.; Kim, K. Facile, Template-Free Synthesis of Stimuli-Responsive Polymer Nanocapsules for Targeted Drug Delivery. *Angew. Chem., Int. Ed.* **2010**, *49*, 4405−4408.
(67) Kim, S.; Yun, G.; Khan, S.; Kim, J.; Murray, J.; Lee, Y. M.; Kim, W. J.; Lee, G.; Kim, S.; Shetty, D.; Kang, J. H.; Kim, J. Y.; Park, K. M.; Kim, K. Cucurbit[6]uril-based polymer nanocapsules as a non-covalent and modular bioimaging platform for multimodal in vivo imaging. *Materials Horizons* **2017**, *4*, 450−455.
(68) Sun, C.; Zhang, H.; Yue, L.; Li, S.; Cheng, Q.; Wang, R. Facile Preparation of Cucurbit[6]uril-Based Polymer Nanocapsules for Targeted Photodynamic Therapy. *ACS Appl. Mater. Interfaces* **2019**, *11*, 22925−22931.
(69) Sun, C.; Yue, L.; Cheng, Q.; Wang, Z.; Wang, R. Macrocycle-Based Polymer Nanocapsules for Hypoxia-Responsive Payload Delivery. *ACS Materials Letters* **2020**, *2*, 266−271.
(70) Sun, C.; Wang, Z.; Yue, L.; Huang, Q.; Lu, S.; Wang, R. ROS-initiated chemiluminescence-driven payload release from macrocycle-based Azo-containing polymer nanocapsules. *J. Mater. Chem. B* **2020**, *8*, 8878−8883.
(71) Griffith, L. G.; Naughton, G. Tissue Engineering−Current Challenges and Expanding Opportunities. *Science* **2002**, *295*, 1009−1014.
(72) Jung, H.; Park, J. S.; Yeom, J.; Selvapalam, N.; Park, K. M.; Oh, K.; Yang, J.-A.; Park, K. H.; Hahn, S. K.; Kim, K. 3D Tissue Engineered Supramolecular Hydrogels for Controlled Chondrogenesis of Human Mesenchymal Stem Cells. *Biomacromolecules* **2014**, *15*, 707−714.
(73) Jang, M.; Kim, H.; Lee, S.; Kim, H. W.; Khedkar, J. K.; Rhee, Y. M.; Hwang, I.; Kim, K.; Oh, J. H. Highly Sensitive and Selective Biosensors Based on Organic Transistors Functionalized with Cucurbit[6]uril Derivatives. *Adv. Funct. Mater.* **2015**, *25*, 4882−4888.
(74) Jin Jeon, Y.; Kim, S.-Y.; Ho Ko, Y.; Sakamoto, S.; Yamaguchi, K.; Kim, K. Novel molecular drug carrier: encapsulation of oxaliplatin in cucurbit[7]uril and its effects on stability and reactivity of the drug. *Organic & Biomolecular Chemistry* **2005**, *3*, 2122−2125.
(75) Chen, Y.; Huang, Z.; Zhao, H.; Xu, J.-F.; Sun, Z.; Zhang, X. Supramolecular Chemotherapy: Cooperative Enhancement of Anti-tumor Activity by Combining Controlled Release of Oxaliplatin and Consuming of Spermine by Cucurbit[7]uril. *ACS Appl. Mater. Interfaces* **2017**, *9*, 8602−8608.
(76) Cao, L.; Hettiarachchi, G.; Briken, V.; Isaacs, L. Cucurbit[7]uril Containers for Targeted Delivery of Oxaliplatin to Cancer Cells. *Angew. Chem., Int. Ed.* **2013**, *52*, 12033−12037.
(77) Sasmal, R.; Das Saha, N.; Pahwa, M.; Rao, S.; Joshi, D.; Inamdar, M. S.; Sheeba, V.; Agasti, S. S. Synthetic Host−Guest Assembly in Cells and Tissues: Fast, Stable, and Selective Bioorthogonal Imaging via Molecular Recognition. *Anal. Chem.* **2018**, *90*, 11305−11314.
(78) Jallinoja, V. I. J.; Carney, B. D.; Zhu, M.; Bhatt, K.; Yazaki, P. J.; Houghton, J. L. Cucurbituril−Ferrocene: Host−Guest Based Pretargeted Positron Emission Tomography in a Xenograft Model. *Bioconjugate Chem.* **2021**, *32*, 1554−1558.
(79) Jallinoja, V. I. J.; Carney, B. D.; Bhatt, K.; Abbriano, C. H.; Schlyer, D. J.; Yazaki, P. J.; Houghton, J. L. Investigation of Copper-64-Based Host−Guest Chemistry Pretargeted Positron Emission Tomography. *Mol. Pharmaceutics* **2022**, *19*, 2268−2278.
(80) Yang, X.; Varini, K.; Godard, M.; Gassiot, F.; Sonnette, R.; Ferracci, G.; Pecqueux, B.; Monnier, V.; Charles, L.; Maria, S.; Hardy, M.; Ouari, O.; Khrestchatisky, M.; Lécorché, P.; Jacquot, G.; Bardelang, D. Preparation and in vitro validation of a cucurbit[7]-uril-peptide conjugate targeting the LDL receptor. *J. Med. Chem.* **2023**, 8844−8857.
(81) Park, K. M.; Murray, J.; Kim, K. Ultrastable Artificial Binding Pairs as a Supramolecular Latching System: A Next Generation Chemical Tool for Proteomics. *Acc. Chem. Res.* **2017**, *50*, 644−646.
(82) Lee, D.-W.; Park, K. M.; Banerjee, M.; Ha, S. H.; Lee, T.; Suh, K.; Paul, S.; Jung, H.; Kim, J.; Selvapalam, N.; Ryu, S. H.; Kim, K. Supramolecular fishing for plasma membrane proteins using an ultrastable synthetic host−guest binding pair. *Nat. Chem.* **2011**, *3*, 154−159.
(83) Murray, J.; Sim, J.; Oh, K.; Sung, G.; Lee, A.; Shrinidhi, A.; Thirunarayanan, A.; Shetty, D.; Kim, K. Enrichment of Specifically Labeled Proteins by an Immobilized Host Molecule. *Angew. Chem., Int. Ed.* **2017**, *56*, 2395−2398.
(84) An, J.; Kim, S.; Shrinidhi, A.; Kim, J.; Banna, H.; Sung, G.; Park, K. M.; Kim, K. Purification of protein therapeutics via high-affinity supramolecular host−guest interactions. *Nature Biomedical Engineering* **2020**, *4*, 1044−1052.
(85) Li, M.; Kim, S.; Lee, A.; Shrinidhi, A.; Ko, Y. H.; Lim, H. G.; Kim, H. H.; Bae, K. B.; Park, K. M.; Kim, K. Bio-orthogonal Supramolecular Latching inside Live Animals and Its Application for in Vivo Cancer Imaging. *ACS Appl. Mater. Interfaces* **2019**, *11*, 43920−43927.
(86) Gong, B.; Choi, B.-K.; Kim, J.-Y.; Shetty, D.; Ko, Y. H.; Selvapalam, N.; Lee, N. K.; Kim, K. High Affinity Host−Guest FRET Pair for Single-Vesicle Content-Mixing Assay: Observation of Flickering Fusion Events. *J. Am. Chem. Soc.* **2015**, *137*, 8908−8911.
(87) Li, M.; Lee, A.; Kim, K. L.; Murray, J.; Shrinidhi, A.; Sung, G.; Park, K. M.; Kim, K. Autophagy Caught in the Act: A Supramolecular FRET Pair Based on an Ultrastable Synthetic Host−Guest Complex Visualizes Autophagosome−Lysosome Fusion. *Angew. Chem., Int. Ed.* **2018**, *57*, 2120−2125.
(88) Dubel, N.; Liese, S.; Scherz, F.; Seitz, O. Exploring the Limits of Bivalency by DNA-Based Spatial Screening. *Angew. Chem., Int. Ed.* **2019**, *58*, 907−911.
(89) Pandey, S.; Kankanamalage, D. V. D. W.; Zhou, X.; Hu, C.; Isaacs, L.; Jayawickramarajah, J.; Mao, H. Chaperone-Assisted Host−Guest Interactions Revealed by Single-Molecule Force Spectroscopy. *J. Am. Chem. Soc.* **2019**, *141*, 18385−18389.
(90) Zhou, X.; Su, X.; Pathak, P.; Vik, R.; Vinciguerra, B.; Isaacs, L.; Jayawickramarajah, J. Host−Guest Tethered DNA Transducer: ATP Fueled Release of a Protein Inhibitor from Cucurbit[7]uril. *J. Am. Chem. Soc.* **2017**, *139*, 13916−13921.
(91) Kankanamalage, D. V. D. W.; Tran, J. H. T.; Beltrami, N.; Meng, K.; Zhou, X.; Pathak, P.; Isaacs, L.; Burin, A. L.; Ali, M. F.; Jayawickramarajah, J. DNA Strand Displacement Driven by Host−Guest Interactions. *J. Am. Chem. Soc.* **2022**, *144*, 16502−16511.
(92) Zielonka, J.; Joseph, J.; Sikora, A.; Hardy, M.; Ouari, O.; Vasquez-Vivar, J.; Cheng, G.; Lopez, M.; Kalyanaraman, B. Mitochondria-Targeted Triphenylphosphonium-Based Compounds: Syntheses, Mechanisms of Action, and Therapeutic and Diagnostic Applications. *Chem. Rev.* **2017**, *117*, 10043−10120.
(93) Bockus, A. T.; Smith, L. C.; Grice, A. G.; Ali, O. A.; Young, C. C.; Mobley, W.; Leek, A.; Roberts, J. L.; Vinciguerra, B.; Isaacs, L.; Urbach, A. R. Cucurbit[7]uril−Tetramethylrhodamine Conjugate for Direct Sensing and Cellular Imaging. *J. Am. Chem. Soc.* **2016**, *138*, 16549−16552.
(94) Webber, M. J.; Appel, E. A.; Vinciguerra, B.; Cortinas, A. B.; Thapa, L. S.; Jhunjhunwala, S.; Isaacs, L.; Langer, R.; Anderson, D. G. Supramolecular PEGylation of biopharmaceuticals. *Proc. Natl. Acad. Sci. U. S. A.* **2016**, *113*, 14189.
(95) Supersaxo, A.; Hein, W. R.; Steffen, H. Effect of Molecular Weight on the Lymphatic Absorption of Water-Soluble Compounds

https://doi.org/10.1021/jacsau.3c00273
JACS Au 2023, 3, 2356−2377

Following Subcutaneous Administration. *Pharm. Res.* **1990**, *7*, 167−169.
(96) Maikawa, C. L.; Smith, A. A. A.; Zou, L.; Roth, G. A.; Gale, E. C.; Stapleton, L. M.; Baker, S. W.; Mann, J. L.; Yu, A. C.; Correa, S.; Grosskopf, A. K.; Liong, C. S.; Meis, C. M.; Chan, D.; Troxell, M.; Maahs, D. M.; Buckingham, B. A.; Webber, M. J.; Appel, E. A. A co-formulation of supramolecularly stabilized insulin and pramlintide enhances mealtime glucagon suppression in diabetic pigs. *Nature Biomedical Engineering* **2020**, *4*, 507−517.
(97) Chen, H.; Chen, Y.; Wu, H.; Xu, J.-F.; Sun, Z.; Zhang, X. Supramolecular polymeric chemotherapy based on cucurbit[7]uril-PEG copolymer. *Biomaterials* **2018**, *178*, 697−705.
(98) Peer, D.; Karp, J. M.; Hong, S.; Farokhzad, O. C.; Margalit, R.; Langer, R. Nanocarriers as an emerging platform for cancer therapy. *Nat. Nanotechnol.* **2007**, *2*, 751−760.
(99) Samanta, S. K.; Quigley, J.; Vinciguerra, B.; Briken, V.; Isaacs, L. Cucurbit[7]uril Enables Multi-Stimuli-Responsive Release from the Self-Assembled Hydrophobic Phase of a Metal Organic Polyhedron. *J. Am. Chem. Soc.* **2017**, *139*, 9066−9074.
(100) Bruns, C. J.; Fujita, D.; Hoshino, M.; Sato, S.; Stoddart, J. F.; Fujita, M. Emergent Ion-Gated Binding of Cationic Host−Guest Complexes within Cationic M12L24 Molecular Flasks. *J. Am. Chem. Soc.* **2014**, *136*, 12027−12034.
(101) Sato, S.; Ikemi, M.; Kikuchi, T.; Matsumura, S.; Shiba, K.; Fujita, M. Bridging Adhesion of a Protein onto an Inorganic Surface Using Self-Assembled Dual-Functionalized Spheres. *J. Am. Chem. Soc.* **2015**, *137*, 12890−12896.
(102) Sun, C.; Zhang, H.; Li, S.; Zhang, X.; Cheng, Q.; Ding, Y.; Wang, L.-H.; Wang, R. Polymeric Nanomedicine with "Lego" Surface Allowing Modular Functionalization and Drug Encapsulation. *ACS Appl. Mater. Interfaces* **2018**, *10*, 25090−25098.
(103) Sun, C.; Wang, Z.; Wang, Z.; Yue, L.; Cheng, Q.; Ye, Z.; Zhang, Q.-W.; Wang, R. Supramolecular nanomedicine for selective cancer therapy via sequential responsiveness to reactive oxygen species and glutathione. *Biomaterials Science* **2021**, *9*, 1355−1362.
(104) Chen, J.; Li, S.; Wang, Z.; Pan, Y.; Wei, J.; Lu, S.; Zhang, Q.-W.; Wang, L.-H.; Wang, R. Synthesis of an AIEgen functionalized cucurbit[7]uril for subcellular bioimaging and synergistic photodynamic therapy and supramolecular chemotherapy. *Chemical Science* **2021**, *12*, 7727−7734.
(105) Chen, J.; Huang, Q.; Wang, Q.; Ding, Y.; Lu, S.; Wang, L.-H.; Li, S.; Wang, R. Supramolecular Luminol−AIEgen Nanoparticles for Deep-Tissue-Inflammation Imaging. *ACS Applied Nano Materials* **2022**, *5*, 5993−6000.
(106) Yue, L.; Yang, K.; Lou, X.-Y.; Yang, Y.-W.; Wang, R. Versatile Roles of Macrocycles in Organic-Inorganic Hybrid Materials for Biomedical Applications. *Matter* **2020**, *3*, 1557−1588.
(107) Yue, L.; Sun, C.; Cheng, Q.; Ding, Y.; Wei, J.; Wang, R. Gold nanorods with a noncovalently tailorable surface for multi-modality image-guided chemo-photothermal cancer therapy. *Chem. Commun.* **2019**, *55*, 13506−13509.
(108) Yue, L.; Yang, K.; Wei, J.; Xu, M.; Sun, C.; Ding, Y.; Yuan, Z.; Wang, S.; Wang, R. Supramolecular Vesicles Based on Gold Nanorods for Precise Control of Gene Therapy and Deferred Photothermal Therapy. *CCS Chemistry* **2021**, *5* (4), 1860−1872.
(109) Yue, L.; Sun, C.; Kwong, C. H. T.; Wang, R. Cucurbit[7]uril-functionalized magnetic nanoparticles for imaging-guided cancer therapy. *J. Mater. Chem. B* **2020**, *8*, 2749−2753.
(110) Cheng, Q.; Yue, L.; Li, J.; Gao, C.; Ding, Y.; Sun, C.; Xu, M.; Yuan, Z.; Wang, R. Supramolecular Tropism Driven Aggregation of Nanoparticles In Situ for Tumor-Specific Bioimaging and Photothermal Therapy. *Small* **2021**, *17*, 2101332.
(111) Ding, Y.-F.; Kwong, C. H. T.; Li, S.; Pan, Y.-T.; Wei, J.; Wang, L.-H.; Mok, G. S. P.; Wang, R. Supramolecular nanomedicine derived from cucurbit[7]uril-conjugated nano-graphene oxide for multi-modality cancer therapy. *Biomaterials Science* **2021**, *9*, 3804−3813.
(112) Zhang, S.; Domínguez, Z.; Assaf, K. I.; Nilam, M.; Thiele, T.; Pischel, U.; Schedler, U.; Nau, W. M.; Hennig, A. Precise supramolecular control of surface coverage densities on polymer micro- and nanoparticles. *Chemical Science* **2018**, *9*, 8575−8581.
(113) Huang, X.; Chen, T.; Mu, N.; Lam, H. W.; Sun, C.; Yue, L.; Cheng, Q.; Gao, C.; Yuan, Z.; Wang, R. Supramolecular micelles as multifunctional theranostic agents for synergistic photodynamic therapy and hypoxia-activated chemotherapy. *Acta Biomaterialia* **2021**, *131*, 483−492.
(114) Zou, L.; Braegelman, A. S.; Webber, M. J. Spatially Defined Drug Targeting by in Situ Host−Guest Chemistry in a Living Animal. *ACS Central Science* **2019**, *5*, 1035−1043.
(115) Gao, C.; Cheng, Q.; Li, J.; Chen, J.; Wang, Q.; Wei, J.; Huang, Q.; Lee, S. M. Y.; Gu, D.; Wang, R. Supramolecular Macrophage-Liposome Marriage for Cell-Hitchhiking Delivery and Immunotherapy of Acute Pneumonia and Melanoma. *Adv. Funct. Mater.* **2021**, *31*, 2102440.
(116) Shi, P.; Ju, E.; Wang, J.; Yan, Z.; Ren, J.; Qu, X. Host−guest recognition on photo-responsive cell surfaces directs cell−cell contacts. *Mater. Today* **2017**, *20*, 16−21.
(117) Gao, C.; Cheng, Q.; Wei, J.; Sun, C.; Lu, S.; Kwong, C. H. T.; Lee, S. M. Y.; Zhong, Z.; Wang, R. Bioorthogonal supramolecular cell-conjugation for targeted hitchhiking drug delivery. *Mater. Today* **2020**, *40*, 9−17.
(118) Cheng, Q.; Xu, M.; Sun, C.; Yang, K.; Yang, Z.; Li, J.; Zheng, J.; Zheng, Y.; Wang, R. Enhanced antibacterial function of a supramolecular artificial receptor-modified macrophage (SAR-Macrophage). *Materials Horizons* **2022**, *9*, 934−941.
(119) Cheng, Q.; Yang, Z.; Quan, X.; Ding, Y.; Li, J.; Wang, Z.; Zhao, Y.; Chen, X.; Wang, R. Tumor polyamines as guest cues attract host-functionalized liposomes for targeting and hunting via a bioorthogonal supramolecular strategy. *Theranostics* **2023**, *13*, 611−620.
(120) Huang, Q.; Cheng, Q.; Zhang, X.; Yin, H.; Wang, L.-H.; Wang, R. Alleviation of Polycation-Induced Blood Coagulation by the Formation of Polypseudorotaxanes with Macrocyclic Cucurbit[7]uril. *ACS Applied Bio Materials* **2018**, *1*, 544−548.
(121) Huang, Q.; Zhao, H.; Shui, M.; Guo, D.-S.; Wang, R. Heparin reversal by an oligoethylene glycol functionalized guanidinocalixarene. *Chemical Science* **2020**, *11*, 9623−9629.
(122) Ding, Y.-F.; Huang, Q.; Quan, X.; Cheng, Q.; Li, S.; Zhao, Y.; Mok, G. S. P.; Wang, R. Supramolecularly functionalized platelets for rapid control of hemorrhage. *Acta Biomaterialia* **2022**, *149*, 248−257.
(123) Ding, Y.-F.; Wei, J.; Quan, X.; Gu, W.; Xi, L.; Zheng, Y.; Zhao, Y.; Luo, J.; Li, S.; Mok, G. S. P.; Wang, R. Hyaluronic acid-based supramolecular medicine with polyamines sequestration capability for cooperative anti-psoriasis. *Carbohydr. Polym.* **2022**, *296*, 119968.
(124) Hennig, A.; Bakirci, H.; Nau, W. M. Label-free continuous enzyme assays with macrocycle-fluorescent dye complexes. *Nat. Methods* **2007**, *4*, 629−632.
(125) Nilam, M.; Karmacharya, S.; Nau, W. M.; Hennig, A. Proton-Gradient-Driven Sensitivity Enhancement of Liposome-Encapsulated Supramolecular Chemosensors. *Angew. Chem., Int. Ed.* **2022**, *61*, e202207950.
(126) Zhang, S.; Assaf, K. I.; Huang, C.; Hennig, A.; Nau, W. M. Ratiometric DNA sensing with a host−guest FRET pair. *Chem. Commun.* **2019**, *55*, 671−674.
(127) Hu, C.; Jochmann, T.; Chakraborty, P.; Neumaier, M.; Levkin, P. A.; Kappes, M. M.; Biedermann, F. Further Dimensions for Sensing in Biofluids: Distinguishing Bioorganic Analytes by the Salt-Induced Adaptation of a Cucurbit[7]uril-Based Chemosensor. *J. Am. Chem. Soc.* **2022**, *144*, 13084−13095.
(128) Das Saha, N.; Pradhan, S.; Sasmal, R.; Sarkar, A.; Beračˇ, C. M.; Kölsch, J. C.; Pahwa, M.; Show, S.; Rozenholc, Y.; Topçu, Z.; Alessandrini, V.; Guibourdenche, J.; Tsatsaris, V.; Gagey-Eilstein, N.; Agasti, S. S. Cucurbit[7]uril Macrocyclic Sensors for Optical Fingerprinting: Predicting Protein Structural Changes to Identifying Disease-Specific Amyloid Assemblies. *J. Am. Chem. Soc.* **2022**, *144*, 14363−14379.
(129) Piller, C. Blots on a field? *Science (New York, NY)* **2022**, *377*, 358−363.

https://doi.org/10.1021/jacsau.3c00273
JACS Au 2023, 3, 2356−2377

(130) Chen, H.; Zhang, J.; Yu, Q.; Chen, Y.; Tan, Y. Hexanoate-Cucurbit[7]uril: Highly Soluble with Controlled Release Ability. *Chemistry – A European Journal* **2020**, *26*, 9445–9448.
(131) Yang, C.; Ke, C.; Liang, W.; Fukuhara, G.; Mori, T.; Liu, Y.; Inoue, Y. Dual Supramolecular Photochirogenesis: Ultimate Stereocontrol of Photocyclodimerization by a Chiral Scaffold and Confining Host. *J. Am. Chem. Soc.* **2011**, *133*, 13786–13789.
(132) Strutt, N. L.; Zhang, H.; Schneebeli, S. T.; Stoddart, J. F. Functionalizing Pillar[n]arenes. *Acc. Chem. Res.* **2014**, *47*, 2631–2642.
(133) Bardelang, D.; Udachin, K. A.; Leek, D. M.; Margeson, J. C.; Chan, G.; Ratcliffe, C. I.; Ripmeester, J. A. Cucurbit[n]urils (n = 5–8): A Comprehensive Solid State Study. *Cryst. Growth Des.* **2011**, *11*, 5598–5614.
(134) Liu, H.-K.; Lin, F.; Yu, S.-B.; Wu, Y.; Lu, S.; Liu, Y.-Y.; Qi, Q.-Y.; Cao, J.; Zhou, W.; Li, X.; Wang, H.; Zhang, D.-W.; Li, Z.-T.; Ma, D. Highly Water-Soluble Cucurbit[8]uril Derivative as a Broad-Spectrum Neuromuscular Block Reversal Agent. *J. Med. Chem.* **2022**, *65*, 16893–16901.
(135) Sawada, T.; Yoshizawa, M.; Sato, S.; Fujita, M. Minimal nucleotide duplex formation in water through enclathration in self-assembled hosts. *Nat. Chem.* **2009**, *1*, 53–56.
(136) Liu, Y.; Zhao, W.; Chen, C.-H.; Flood, A. H. Chloride capture using a C–H hydrogen-bonding cage. *Science* **2019**, *365*, 159–161.
(137) Yawer, M. A.; Havel, V.; Sindelar, V. A Bambusuril Macrocycle that Binds Anions in Water with High Affinity and Selectivity. *Angew. Chem., Int. Ed.* **2015**, *54*, 276–279.
(138) Tromans, R. A.; Carter, T. S.; Chabanne, L.; Crump, M. P.; Li, H.; Matlock, J. V.; Orchard, M. G.; Davis, A. P. A biomimetic receptor for glucose. *Nat. Chem.* **2019**, *11*, 52–56.
(139) Wheate, N. J.; Day, A. I.; Blanch, R. J.; Arnold, A. P.; Cullinane, C.; Grant Collins, J. Multi-nuclear platinum complexes encapsulated in cucurbit[n]uril as an approach to reduce toxicity in cancer treatment. *Chem. Commun.* **2004**, 1424–1425.
(140) Liu, W.; Samanta, S. K.; Smith, B. D.; Isaacs, L. Synthetic mimics of biotin/(strept)avidin. *Chem. Soc. Rev.* **2017**, *46*, 2391–2403.
(141) Shetty, D.; Khedkar, J. K.; Park, K. M.; Kim, K. Can we beat the biotin–avidin pair?: cucurbit[7]uril-based ultrahigh affinity host–guest complexes and their applications. *Chem. Soc. Rev.* **2015**, *44*, 8747–8761.
(142) Dey, S.; Fan, C.; Gothelf, K. V.; Li, J.; Lin, C.; Liu, L.; Liu, N.; Nijenhuis, M. A. D.; Saccà, B.; Simmel, F. C.; Yan, H.; Zhan, P. DNA origami. *Nature Reviews Methods Primers* **2021**, *1*, 13.
(143) Huang, K.; Yang, D.; Tan, Z.; Chen, S.; Xiang, Y.; Mi, Y.; Mao, C.; Wei, B. Self-Assembly of Wireframe DNA Nanostructures from Junction Motifs. *Angew. Chem., Int. Ed.* **2019**, *58*, 12123–12127.
(144) Evans, C. G.; Winfree, E. Physical principles for DNA tile self-assembly. *Chem. Soc. Rev.* **2017**, *46*, 3808–3829.
(145) Dalgarno, S. J.; Power, N. P.; Atwood, J. L. Metallo-supramolecular capsules. *Coord. Chem. Rev.* **2008**, *252*, 825–841.
(146) Winter, A.; Schubert, U. S. Synthesis and characterization of metallo-supramolecular polymers. *Chem. Soc. Rev.* **2016**, *45*, 5311–5357.
(147) Hooper, C. A. J.; Cardo, L.; Craig, J. S.; Melidis, L.; Garai, A.; Egan, R. T.; Sadovnikova, V.; Burkert, F.; Male, L.; Hodges, N. J.; Browning, D. F.; Rosas, R.; Liu, F.; Rocha, F. V.; Lima, M. A.; Liu, S.; Bardelang, D.; Hannon, M. J. Rotaxanating Metallo-supramolecular Nano-cylinder Helicates to Switch DNA Junction Binding. *J. Am. Chem. Soc.* **2020**, *142*, 20651–20660.
(148) August, D. P.; Dryfe, R. A. W.; Haigh, S. J.; Kent, P. R. C.; Leigh, D. A.; Lemonnier, J.-F.; Li, Z.; Muryn, C. A.; Palmer, L. I.; Song, Y.; Whitehead, G. F. S.; Young, R. J. Self-assembly of a layered two-dimensional molecularly woven fabric. *Nature* **2020**, *588*, 429–435.
(149) Wang, J.; Wicher, B.; Méndez-Ardoy, A.; Li, X.; Pecastaings, G.; Buffeteau, T.; Bassani, D. M.; Maurizot, V.; Huc, I. Loading Linear Arrays of CuII Inside Aromatic Amide Helices. *Angew. Chem., Int. Ed.* **2021**, *60*, 18461–18466.
(150) Tam, A. Y.-Y.; Yam, V. W.-W. Recent advances in metallogels. *Chem. Soc. Rev.* **2013**, *42*, 1540–1567.
(151) Leigh, D. A.; Pritchard, R. G.; Stephens, A. J. A Star of David catenane. *Nat. Chem.* **2014**, *6*, 978–982.
(152) August, D. P.; Borsley, S.; Cockroft, S. L.; della Sala, F.; Leigh, D. A.; Webb, S. J. Transmembrane Ion Channels Formed by a Star of David [2]Catenane and a Molecular Pentafoil Knot. *J. Am. Chem. Soc.* **2020**, *142*, 18859–18865.
(153) Kassem, S.; van Leeuwen, T.; Lubbe, A. S.; Wilson, M. R.; Feringa, B. L.; Leigh, D. A. Artificial molecular motors. *Chem. Soc. Rev.* **2017**, *46*, 2592–2621.
(154) Yin, H.; Rosas, R.; Gigmes, D.; Ouari, O.; Wang, R.; Kermagoret, A.; Bardelang, D. Metal Actuated Ring Translocation Switches in Water. *Org. Lett.* **2018**, *20*, 3187–3191.
(155) Cheng, Q.; Yin, H.; Rosas, R.; Gigmes, D.; Ouari, O.; Wang, R.; Kermagoret, A.; Bardelang, D. A pH-driven ring translocation switch against cancer cells. *Chem. Commun.* **2018**, *54*, 13825–13828.
(156) Yang, X.; Cheng, Q.; Monnier, V.; Charles, L.; Karoui, H.; Ouari, O.; Gigmes, D.; Wang, R.; Kermagoret, A.; Bardelang, D. Guest Exchange by a Partial Energy Ratchet in Water. *Angew. Chem., Int. Ed.* **2021**, *60*, 6617–6623.
(157) Goodsell, D. S. *The machinery of life*. Springer, 2009.
(158) Dang, D. T.; Schill, J.; Brunsveld, L. Cucurbit[8]uril-mediated protein homotetramerization. *Chemical Science* **2012**, *3*, 2679–2684.
(159) Biedermann, F.; Hathazi, D.; Nau, W. M. Associative chemosensing by fluorescent macrocycle–dye complexes – a versatile enzyme assay platform beyond indicator displacement. *Chem. Commun.* **2015**, *51*, 4977–4980.
(160) Cheng, Q.; Li, S.; Ma, Y.; Yin, H.; Wang, R. pH-Responsive supramolecular DOX-dimer based on cucurbit[8]uril for selective drug release. *Chin. Chem. Lett.* **2020**, *31*, 1235–1238.
(161) Appel, E. A.; Forster, R. A.; Rowland, M. J.; Scherman, O. A. The control of cargo release from physically crosslinked hydrogels by crosslink dynamics. *Biomaterials* **2014**, *35*, 9897–9903.

https://doi.org/10.1021/jacsau.3c00273
JACS Au 2023, 3, 2356–2377